Lovejoy, C. A., Lock, K., Yenamandra, A., and Cortez, D. (2006). DDB1 maintains genome integrity through regulation of Cdt1. Mol. Cell. Biol. *26*, 7977–7990.

Mailand, N., and Diffley, J. F. (2005). CDKs promote DNA replication origin licensing in human cells by protecting Cdc6 from APC/C-dependent proteolysis. Cell *122*, 915–926.

Maiorano, D., Moreau, J., and Méchali, M. (2000). XCDT1 is required for the assembly of pre-replicative complexes in *Xenopus laevis*. Nature *404*, 622–625.

McGarry, T. J., and Kirschner, M. W. (1998). Geminin, an inhibitor of DNA replication, is degraded during mitosis. Cell *93*, 1043–1053.

Mihaylov, I. S., Kondo, T., Jones, L., Ryzhikov, S., Tanaka, J., Zheng, J., Higa, L. A., Minamino, N., Cooley, L., and Zhang, H. (2002). Control of DNA replication and chromosome ploidy by geminin and cyclin A. Mol. Cell. Biol. *22*, 1868–1880.

Nguyen, V. Q., Co, C., and Li, J. J. (2001). Cyclin-dependent kinases prevent DNA re-replication through multiple mechanisms. Nature *411*, 1068–1073.

Nishitani, H., Lygerou, Z., Nishimoto, T., and Nurse, P. (2000). The Cdt1 protein is required to license DNA for replication in fission yeast. Nature *404*, 625–628.

Nishitani, H., Taraviras, S., Lygerou, Z., and Nishimoto, T. (2001). The human licensing factor for DNA replication Cdt1 accumulates in G1 and is destabilized after initiation of S-phase. J. Biol. Chem. *276*, 44905–44911.

Nishitani, H., Lygerou, Z., and Nishimoto, T. (2004). Proteolysis of DNA replication licensing factor Cdt1 in S-phase is performed independently of geminin through its N-terminal region. J. Biol. Chem. *279*, 30807–30816.

Nishitani, H. *et al.* (2006). Two E3 ubiquitin ligases, SCF-Skp2 and DDB1-Cul4, target human Cdt1 for proteolysis. EMBO J. *25*, 1126–1136.

Petersen, B. O., Lukas, J., Sorensen, C. S., Bartek, J., and Helin, K. (1999). Phosphorylation of mammalian CDC6 by cyclin A/CDK2 regulates its subcellular localization. EMBO J. *18*, 396–410.

Petersen, B. O. *et al.* (2000). Cell cycle-and cell growth-regulated proteolysis of mammalian CDC6 is dependent on APC-CDH1. Genes Dev. *14*, 2330–2343.

Pfleger, C. M., and Kirschner, M. W. (2000). The KEN box: an APC recognition signal distinct from the D box targeted by Cdh1. Genes Dev. *14*, 655–665.

Pines, J. (2006). Mitosis: a matter of getting rid of the right protein at the right time. Trends Cell Biol. *16*, 55–63.

Poot, R. A., Bozhenok, L., van den Berg, D. L., Steffensen, S., Ferreira, F., Grimaldi, M., Gilbert, N., Ferreira, J., and Varga-Weisz, P. D. (2004). The Williams syndrome transcription factor interacts with PCNA to target chromatin remodeling by ISWI to replication foci. Nat. Cell Biol. *6*, 1236–1244.

Sansam, C. L., Shepard, J. L., Lai, K., Ianari, A., Danielian, P. S., Amsterdam, A., Hopkins, N., and Lees, J. A. (2006). DTL/CDT2 is essential for both CDT1 regulation and the early G2/M checkpoint. Genes Dev. *20*, 3117–3129.

Schaper, S., Fromont-Racine, M., Linder, P., de la Cruz, J., Namane, A., and Yaniv, M. (2001). A yeast homolog of chromatin assembly factor 1 is involved in early ribosome assembly. Curr. Biol. *11*, 1885–1890.

Senga, T., Sivaprasad, U., Zhu, W., Park, J. H., Arias, E. E., Walter, J. C., and Dutta, A. (2006). PCNA is a cofactor for Cdt1 degradation by CUL4/DDB1-mediated N-terminal ubiquitination. J. Biol. Chem. *281*, 6246–6252.

Simmons, D. T., Gai, D., Parsons, R., Debes, A., and Roy, R. (2004). Assembly of the replication initiation complex on SV40 origin DNA. Nucleic Acids Res. *32*, 1103–1112.

Sorensen, C. S., Lukas, C., Kramer, E. R., Peters, J. M., Bartek, J., and Lukas, J. (2000). Nonperiodic activity of the human anaphase-promoting complex—Cdh1 ubiquitin ligase results in continuous DNA synthesis uncoupled from mitosis. Mol. Cell. Biol. *20*, 7613–7623.

Sugimoto, N., Tatsumi, Y., Tsurumi, T., Matsukage, A., Kiyono, T., Nishitani, H., and Fujita, M. (2004). Cdt1 phosphorylation by cyclin A-dependent kinases negatively regulates its function without affecting geminin binding. J. Biol. Chem. *279*, 19691–19697.

Tada, S., Li, A., Maiorano, D., Méchali, M., and Blow, J. J. (2001). Repression of origin assembly in metaphase depends on inhibition of RLF-B/Cdt1 by geminin. Nat. Cell Biol. *3*, 107–113.

Taguchi, S., Honda, K., Sugiura, K., Yamaguchi, A., Furukawa, K., and Urano, T. (2002). Degradation of human Aurora-A protein kinase is mediated by hCdh1. FEBS Lett. *519*, 59–65.

Takeda, D. Y., Parvin, J. D., and Dutta, A. (2005). Degradation of Cdt1 during S phase is Skp2-independent and is required for efficient progression of mammalian cells through S phase. J. Biol. Chem. *280*, 23416–23423.

Tanaka, S., and Diffley, J. F. (2002). Interdependent nuclear accumulation of budding yeast Cdt1 and Mcm2–7 during G1 phase. Nat. Cell Biol. *4*, 198–207.

Tatsumi, Y., Sugimoto, N., Yugawa, T., Narisawa-Saito, M., Kiyono, T., and Fujita, M. (2006). Deregulation of Cdt1 induces chromosomal damage without rereplication and leads to chromosomal instability. J. Cell Sci. *119*, 3128–3140.

Tsurimoto, T. (1999). PCNA binding proteins. Front. Biosci. *4*, D849–D858.

Vaziri, C., Saxena, S., Jeon, Y., Lee, C., Murata, K., Machida, Y., Wagle, N., Hwang, D. S., and Dutta, A. (2003). A p53-dependent checkpoint pathway prevents rereplication. Mol. Cell *11*, 997–1008.

Vodermaier, H. C. (2004). APC/C and SCF: controlling each other and the cell cycle. Curr. Biol. *14*, R787–R796.

Wang, J. C. (1996). DNA topoisomerases. Annu. Rev. Biochem. *65*, 635–692.

Wei, W., Ayad, N. G., Wan, Y., Zhang, G. J., Kirschner, M. W., and Kaelin, W. G., Jr. (2004). Degradation of the SCF component Skp2 in cell-cycle phase G1 by the anaphase-promoting complex. Nature *428*, 194–198.

Wohlschlegel, J. A., Dwyer, B. T., Dhar, S. K., Cvetic, C., Walter, J. C., and Dutta, A. (2000). Inhibition of eukaryotic DNA replication by geminin binding to Cdt1. Science *290*, 2309–2312.

Xouri, G., Ligerou, Z., Nishitani, H., Pachnis, V., Nurse, P., and Taraviras, S. (2004). Cdt1 and geminin are down-regulated upon cell cycle exit and are over-expressed in cancer-derived cell lines. Eur. J. Biochem. *271*, 3368–3378.

Yanagi, K., Mizuno, T., You, Z., and Hanaoka, F. (2002). Mouse geminin inhibits not only Cdt1-MCM6 interactions but also a novel intrinsic Cdt1 DNA binding activity. J. Biol. Chem. *277*, 40871–40880.

Zhong, W., Feng, H., Santiago, F. E., and Kipreos, E. T. (2003). CUL-4 ubiquitin ligase maintains genome stability by restraining DNA-replication licensing. Nature *423*, 885–889.

Zhou, J., Chau, C. M., Deng, Z., Shiekhattar, R., Spindler, M.-P., Schepers, A., and Lieberman, P. M. (2005). Cell cycle regulation of chromatin at an origin of DNA replication. EMBO J. *24*, 1406–1417.

Available online at www.sciencedirect.com
ScienceDirect
Biochemical and Biophysical Research Communications 368 (2008) 536–542
BBRC
www.elsevier.com/locate/ybbrc

Phosphorylation of Runx1 at Ser249, Ser266, and Ser276 is dispensable for bone marrow hematopoiesis and thymocyte differentiation

Masashi Tachibana [a,b], Chieko Tezuka [a], Sawako Muroi [a,c], Sogo Nishimoto [a], Takuo Katsumoto [d], Atsushi Nakajima [b], Issay Kitabayashi [d], Ichiro Taniuchi [a,c,*]

[a] *Laboratory for Transcriptional Regulation, RIKEN Research Center for Allergy and Immunology, 1-7-22 Suehiro-cho, Tsurumi-ku, Yokohama 230-0045, Japan*
[b] *Gastroenterology Division, Yokohama City University School of Medicine, 3-9 Fukuura, Kanazawa-ku, Yokohama 236-0004, Japan*
[c] *PRESTO, Japan Science and Technology Agency, 4-1-8 Honcho, Kawaguchi, Saitama 332-0012, Japan*
[d] *Molecular Oncology Division, National Cancer Center Research Institute, 5-1-1 Tsukiji, Chuo-ku, Tokyo 104-0045, Japan*

Received 29 December 2007
Available online 6 February 2008

Abstract

Runx1, one of three mammalian runt-domain transcription factor family proteins, is essential for definitive hematopoiesis. Based on transfection assays, phosphorylation of Runx1 at the three serine residues, Ser249, Ser266, and Ser276, was thought to be important for trans-activation activity of Runx1. By using "knock-in" gene targeting, we generated mouse strains expressing mutant Runx1 protein that harbored a combined serine-to-alanine substitution at either of two residues, Ser249/Ser266 or Ser249/Ser276. Either mutation resulted in a lack of major phosphorylated form of Runx1. However, while loss of definitive hematopoiesis and impaired thymocyte differentiation was observed following the loss of Runx1, these phenotypes were rescued in those mice lacking the major phosphorylated form of Runx1. These results not only challenge the predicted regulation of Runx1 activity by phosphorylation at these serine residues, but also reaffirm the effectiveness of "knock-in" mutagenesis as a powerful tool for addressing the physiological relevance of post-translation modifications.

Keywords: Runx1; Phosphorylation; Hematopoiesis; Lymphocyte differentiation; Knock-in mutagenesis; Transcription factor; Post-translational modifications

Runx1 (also known as AML1, CBFα1 or PEBP2αB) belongs to the runt-domain transcription factor family, and functions as α-subunit of the Runx complexes following dimerization with the non-DNA binding obligatory β-subunit Cbfβ [1]. Genetic studies in several species have revealed that Runx complexes engage in a variety of biological activities during the differentiation of many cell types [2–5]. For instances, Runx1 has been shown to be essential for definitive hematopoiesis [6,7]. On the other hand, human *RUNX1/AML1* gene remains the most frequent target of leukemia-associated chromosomal translocation or mutations observed in acute myeloid leukemia (AML) patients [8–10]. It is thus important to identify mechanisms that regulate Runx1 function to further understand the physiological and pathological contribution of Runx1 in hematopoiesis and leukemia, respectively.

In addition to the regulation of their expression levels, the biological activities of transcription factors may be regulated by various post-translational modifications. Runx1 protein has been shown to be phosphorylated by at least two kinase families, mitogen-activated protein kinase (MAPK) and homeodomain-interacting protein kinase (HIPK). Putative amino acid residues destined to be phosphorylated by MAPKs or HIPKs were mapped to the Runx1 protein residues Ser249 and Ser266 or Ser249 and

* Corresponding author. Fax: +81 45 503 7043.
E-mail address: taniuchi@rcai.riken.jp (I. Taniuchi).

0006-291X/$ - see front matter © 2008 Elsevier Inc. All rights reserved.
doi:10.1016/j.bbrc.2008.01.124

Ser276, respectively [11–13]. In transfection assays, the mutations converting these serine residues to alanine residues diminished the Runx1-mediated activation of reporter genes [12–14]. Given that these serine residues are located in close proximity to the trans-activation domain of Runx1, phosphorylation of Runx1 protein has been postulated to act as an important regulatory mechanism enhancing the trans-activation activity of Runx1.

Consistently, impaired hematopoiesis in mice deficient for both HIPK1 and HIPK2 has suggested a possible involvement of HIPK-mediated Runx1 phosphorylation in Runx1-dependent programming of hematopoiesis [11]. Runx1 has also been shown to regulate thymocyte differentiation [15,16] in part through binding to the TCRβ enhancer (Eβ) [17]. Interestingly phorbol ester-induced activation of Eβ by Runx1 is dependent upon the phosphorylation of several serine/threonine residues including Ser276 [13]. In addition, Runx1 is necessary for the efficient positive selection of $CD4^+CD8^+$ DP thymocytes [16], a process influenced by MAPK pathway downstream of TCR signaling, suggesting that MAPK-dependent phosphorylation of Runx1 plays an important role in Runx1-mediated gene regulation in DP thymocytes. Thus, increasing evidence suggests that phosphorylation at Ser249, Ser266 or Ser276 plays an important role in the regulation of Runx1 activity.

In this study, we introduced two types of mutations into the murine *Runx1* locus in order to target serine-to-alanine substitutions at either of two residues, Ser249/Ser266 or Ser249/Ser276. Unexpectedly, phenotypes resulting from Runx1-deficiency that occurs during hematopoiesis and lymphopoiesis were rescued in those mice, although loss of phosphorylation at the above-mentioned serine residues resulted in a loss of the major phosphorylated form of Runx1. Thus Runx1 protein maintains an activity level sufficient for normal hematopoiesis, even in the absence of major phosphorylation.

Materials and methods

Generation of $Runx1^{PM12A}$ and $Runx1^{PM13A}$ alleles. A genomic DNA fragment used to construct the targeting vectors was obtained from the phage library (Stratagene). Both the 5′ long homology region and the 3′ short homology region were PCR amplified with an LA-PCR kit (TAKARA). The genomic DNA fragments harboring mutations for serine-to-alanine substitutions at the proposed positions were generated by employing overlapping PCR techniques. These three DNA fragments were sequentially ligated into pBluescript vector harboring *neomycin*-resistant gene and HSV-*thymidine kinase* gene in order to generate the targeting vectors. Transfection into E14 ES cells and generation of chimera mice were performed as previously described [15].

Immunoblot analysis and antibody generation. Cell lysates were prepared by sonication in a lysis buffer containing 100 mM Tris–HCl (pH 7.4), 300 mM NaCl, 2 mM EDTA, 2% Triton X-100, 0.2% SDS, 0.2% sodium deoxycholate, a protease inhibitor cocktail (Roche), and phosphatase inhibitor cocktail (Pierce). Lysates were separated by 10% SDS–PAGE and transferred onto polyvinylidene difluoride membranes (Amersham Biosciences). Membranes incubated with the first antibody were reacted with HRP-labeled anti-rabbit IgG (Amersham Biosciences), and then visualized with an ECL kit (GE Healthcare). An antibody against the N-terminal end of the distal promoter-derived Runx1 was generated by immunizing rabbits with the peptides, MASDSIFESFPSYPQCFMRDA. The antibody that reacted with Runx1 phosphorylated Ser249 was described previously [11], while that which reacted with Runx1 phosphorylated Ser276 will be described elsewhere by I.K.

Calf intestinal alkaline phosphatase (CIAP) treatment. Immunoprecipitation was performed using a Rabbit IgG TrueBlot Set (eBioscience) according to the manufacturer's protocol. Immunoprecipitated lysates bound to beads were incubated with 1 U/μL CIAP (Promega) for 30 min at 37 °C. After washing twice, samples were boiled with Laemmli sample buffer (Bio-Rad) to release proteins from beads.

Flow cytometry analyses. All antibodies used for flow cytometry were from BD Pharmingen or eBioscience. PE-conjugated αGalCer/CD1d-dimer was kindly provided by Dr. M. Taniguchi (RIKEN, RCAI). For surface staining, cells were incubated for 15–20 min at 4 °C with the corresponding cocktail of fluorescent-labeled antibodies. Data were acquired with a FACS Calibur (BD Biosciences) and were analyzed with FlowJo software (Tree Star Inc.).

Cell preparation. Thymocyte subsets were purified by electrical cell sorting using FACS Vantage (BD Biosciences). $CD43^+$ bone marrow cells and $B220^+$ splenic B cells were prepared using MACS beads (Miltenyi Biotec). For NKT cell preparation, liver cells were suspended in 33% Percoll solution (Amersham Biosciences) and then centrifuged for 20 min at room temperature. Pellets were used as liver mononuclear cells for subsequent study after lysing red blood cells.

Results and discussion

Generation of $Runx1^{PM12A}$ and $Runx1^{PM13A}$ mouse strains

Murine Runx1 protein has been shown to be phosphorylated at Ser249 and Ser266 mainly by Erk [12], while Ser249 and Ser276 residues are phosphorylated by HIPKs [11] (Fig. 1B). We therefore constructed the targeting vectors to introduce mutations leading to serine-to-alanine substitutions at murine Runx1 residues Ser249 and Ser266 (S249/266A) or at Ser249 and Ser276 (S249/276A) (Fig. 1A and B). The constructed mutations of the *Runx1* gene for S249/266A or S249/276A substitution are referred to hereafter as phosphorylation mutation 12A (PM12A) or PM13A, respectively.

After confirming a homologous recombination in ES cells by Southern blot, followed by excision of the *Neo* gene by transient transfection of *Cre* recombinase (Fig. 1A and Supplementary Fig. S1), we generated chimera mice from suitable ES cell clones via transmission of their mutations, thereby establishing the mouse strains $Runx1^{PM12A}$ and $Runx1^{PM13A}$ (Supplementary Fig. S1). Mice homozygous for either mutation were born at the expected frequency rate and grew normally. DNA sequencing confirmed that the mutant animals harbored the constructed mutations (Fig. 1C). Given that Runx1-deficient embryos die around 11.5 dpc by massive hemorrhage [6,7], the normal growth of $Runx1^{PM12A/PM12A}$ and $Runx1^{PM13A/PM13A}$ mice indicates that Runx1 function essential to early mouse development is independent of phosphorylation at residues Ser249, Ser266 or Ser276.

Biochemical characterization of $Runx1^{S249/266A}$ and $Runx1^{S249/276A}$ protein

Using an antibody that recognizes the N-terminal end of Runx1, immunoblot analyses detected Runx1 protein

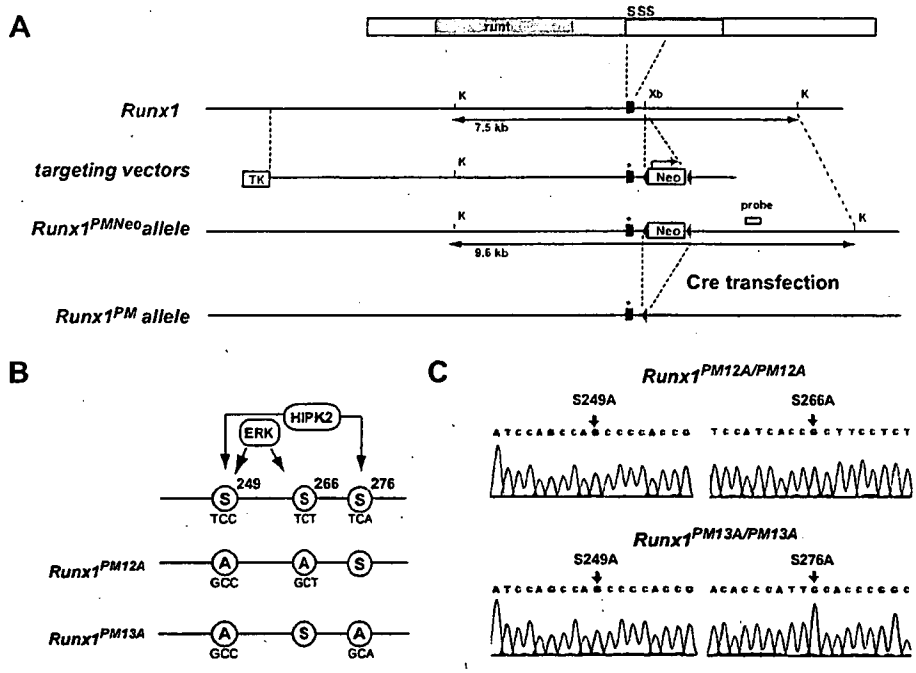

Fig. 1. Generation of mutant mice expressing Runx1$^{S249/266A}$ or Runx1$^{S249/276A}$ mutant Runx1 protein. (A) Structure of the *Runx1* locus, the targeting vectors and the targeted mutant *Runx1* locus. The black box, the black box marked with an asterisk and the triangle represent exon, mutated exon and loxP sequences, respectively. The open boxes marked with TK or Neo indicate *thimidine kinase* genes and *neomycin*-resistant genes, respectively. The DNA fragment used in the Southern blot analysis is indicated as a gray box. Restriction enzyme sites shown are KpnI (K) and XbaI (Xb). (B) Three phosphorylation serine residues of Runx1 and its putative kinases. The constructed DNA mutations *Runx1*^{PM12A} and *Runx1*^{PM13A} for serine-to-alanine substitutions on both Ser249 and Ser266 (S249/266A) or on both Ser249 and Ser276 (S249/276A) residues are indicated, respectively. (C) DNA sequences from mice homozygous for either *Runx1*^{PM12A} or *Runx1*^{PM13A} confirmed that the constructed mutations were correctly targeted into the *Runx1* locus.

expressed at two positions (Fig. 2A). However, only the more rapidly migrating Runx1 protein was detected in thymocytes from *Runx1*$^{PM12A/PM12A}$ and *Runx1*$^{PM13A/PM13A}$ mice (Fig. 2A). An antibody that reacts specifically with Runx1 phosphorylated Ser249 detected Runx1 protein at the position corresponding to the more slowly migrating Runx1 in *wild-type* thymocytes, while there were no detectable signals in the cell lysates of *Runx1*$^{PM12A/PM12A}$ and *Runx1*$^{PM13A/PM13A}$ mice (Fig. 2A). In similar fashion, an antibody against Runx1-derived peptide including phosphorylated Ser276 (anti-p-S^{276} Runx1 antibody) mainly reacted with the more slowly migrating Runx1 in control sample, while no reactive protein was detected in thymocytes from *Runx1*$^{PM13A/PM13A}$ mice (Fig. 2A). The anti-p-S^{276} Runx1 antibody still reacted with Runx1$^{S249/266A}$ protein from *Runx1*$^{PM12A/PM12A}$ mice, indicating that phosphorylation at Ser276 residues is independent from that occurring at the Ser249 and Ser266 residues.

To examine whether the Runx1$^{S249/276A}$ protein is phosphorylated at other residues, we treated *wild-type* Runx1 or Runx1$^{S249/276A}$ protein with calf intestinal alkaline phosphatase (CIAP) prior to immunoblot analyses (Fig. 2B). Disappearance of the more slowly migrating Runx1 protein by CIAP treatment confirmed that Runx1 protein in the upper position undergoes phosphorylation. Furthermore, the position of the CIAP-treated Runx1 protein was slightly lower than that of the more rapidly migrating Runx1. Similar changes in molecular weight following CIAP treatment were observed in Runx1$^{S249/276A}$ protein. These results indicate that Runx1 protein in thymocytes is phosphorylated to differing extents, appearing as two distinct bands (i.e., the major and minor phosphorylated forms) in immunoblot analyses.

Runx1 protein was detected as two bands in CD4$^-$CD8$^-$ DN thymocytes negative for αβTCR expression as well as in CD4$^+$CD8$^+$ DP thymocyte positive for αβTCR expression (Fig. 2C), indicating that natural phosphorylation of Runx1 protein would occur independently from TCR engagement. Runx1 expression in CD43$^+$ bone marrow cells containing hematopoietic stem/progenitors was almost undetectable, although inactivation of the *Runx1* gene affected the differentiation and homeostasis of these cells [6,18]. In contrast, Runx1 expression was easily detected in splenic B220$^+$ B lymphocytes as double bands, the upper one of which was lacked in cells from *Runx1*$^{PM13A/PM13A}$ mice (Fig. 2C). Thus major phosphorylation of Runx1 also occurs in B lymphocytes.

Collectively, these biochemical results indicate that the Ser249, Ser266, and Ser276 residue are physiological phosphorylation sites. Runx1 protein in lymphocytes is naturally phosphorylated to distinct degrees, thus comprising major and minor phosphorylated forms. Phosphorylation at Ser249 would be essential for sequential

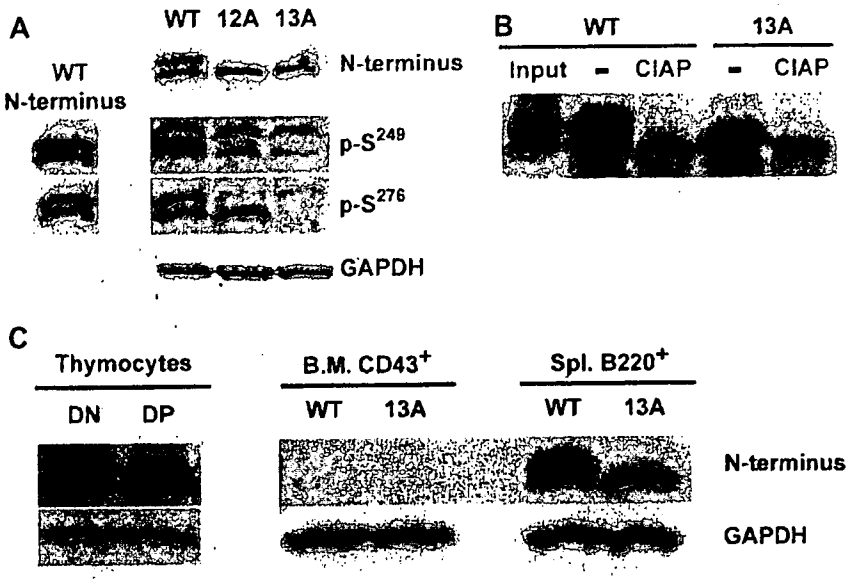

Fig. 2. Loss of the major phosphorylated form of Runx1 in *Runx1*$^{PM12A/PM12A}$ and *Runx1*$^{PM13A/PM13A}$ mice. (A) Immunoblot analyses of total thymocytes from *wild-type* (WT), *Runx1*$^{PM12A/PM12A}$ (12A) and *Runx1*$^{PM13A/PM13A}$ (13A) mice with three different antibodies recognizing either N-terminal end (N-terminus), phosphorylated Ser249 (p-S^{249}) or phosphorylated Ser276 (p-S^{276}) of murine Runx1 protein. Position of WT Runx1 protein detected by anti-N-terminus antibody is indicated as a reference at the left of middle and lower panel. GAPDH expressions are shown as a loading control. (B) Calf intestinal alkaline phosphatase (CIAP) treatment indicated that the most slowly migrating Runx1 constitutes a major phosphorylated form of Runx1, one that is absent in *Runx1*$^{PM13A/PM13A}$ mice. (C) Immunoblot analyses of Runx1 with anti-N-terminus Runx1 in CD4$^-$CD8$^-$ DN thymocytes (DN) and CD4$^+$CD8$^+$ DP thymocytes (DP) from wild-type mice (left panel), as well as CD43$^+$ bone marrow cells (B.M. CD43$^+$) and B220$^+$ splenic cells (Spl. B220$^+$) from wild-type (WT) and *Runx1*$^{PM13A/PM13A}$ (13A) mice.

phosphorylation at other residues when generating the major phosphorylated form of Runx1.

Phosphorylation of Runx1 at Ser249, Ser266, and Ser276 is not essential for early hematopoiesis and myeloid cell differentiation

We next examined the effect of *Runx1*^{PM12A} or *Runx1*^{PM13A} mutation on hematopoietic cell differentiation. In adult bone marrow, hematopoietic stem/progenitor cells and common lymphoid progenitors (CLPs) are included in lineage (Lin)$^-$IL-7Rα$^-$c-Kit$^+$Sca-1$^+$ cells and Lin$^-$IL-7R$^+$c-Kit^{low}Sca-1^{low} subset, respectively. The percentages of these populations in *Runx1*$^{PM12A/PM12A}$ and *Runx1*$^{PM13A/PM13A}$ mice are compatible with those of *wild-type* mice. Similarly common myeloid progenitors (CMPs, Lin$^-$Sca-1$^-$c-Kit$^+$CD34$^+$FcγRIII/II^{lo}), granulocyte/macrophage progenitors (GMPs, Lin$^-$Sca-1$^-$c-Kit$^+$CD34$^+$FcγRIII/II$^+$) and megakaryocyte/erythroid progenitors (MEPs, Lin$^-$Sca-1$^-$c-Kit$^+$CD34$^+$FcγRIII/II$^{lo/-}$) were normally present in *Runx1*$^{PM12A/PM12A}$ and *Runx1*$^{PM13A/PM13A}$ mice (Fig. 3A). Consistent with normal development of progenitor cells, there were no significant changes in differentiation of megakaryocyte, monocytes, granulocytes or erythroblast in bone marrow (Supplementary Fig. S2). Finally the erythroid or myeloid colony-forming activity of bone marrow cells in methylcellulose medium was not influenced by *Runx1*^{PM12A} or *Runx1*^{PM13A} mutation (Fig. 3B).

These results indicate that phosphorylation of Runx1 at Ser249, Ser266, and Ser276 is nonessential for Runx1 function required in early hematopoiesis. Considering the fact that HIPKs have been shown to be important in early hematopoiesis [11], substrate or interacting molecules other than Runx1 may exist in the HIPK-dependent regulation of early hematopoiesis.

Phosphorylation of Runx1 at Ser249, Ser266, and Ser276 is not essential for thymocyte differentiation

Inactivation of the *Runx1* gene in early thymocytes progenitors by *Lck-Cre* transgene partially inhibited thymocyte development. We therefore examined thymocyte differentiation in *Runx1*$^{PM12A/PM12A}$ and *Runx1* $^{PM13A/PM13A}$ mice. A decrease in the number of thymocytes concomitant with the accumulation of CD4$^-$CD8$^-$ DN thymocytes, as observed in *Runx1*$^{fl/fl}$: *Lck-Cre* mice [15], was not observed in these two mutant mice (Fig. 4A and B). CD4 repression in CD4$^-$CD8$^-$ DN thymocytes is regulated by the intronic *Cd4* silencer, whose activity requires the binding of Runx1 protein [15]. However, CD4 expression levels in TCRβ$^-$CD8$^-$CD25$^+$ populations corresponding to DN3 thymocytes were normal in *Runx1*$^{PM12A/PM12A}$ and *Runx1* $^{PM13A/PM13A}$ mice (Supplementary Fig. S3).

Erk functions downstream of TCR signaling and plays an important role in the selection of CD4$^+$CD8$^+$DP thymocytes [19]. As Runx1 has been shown not only to be a substrate of Erk [12] but also important for positive selec-

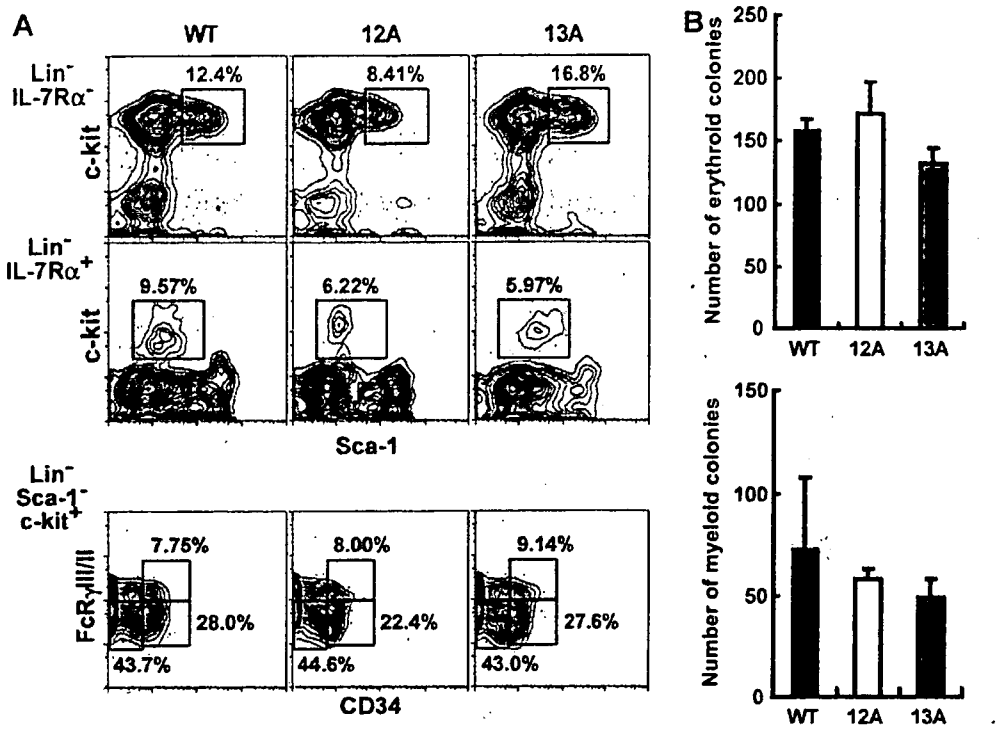

Fig. 3. Phosphorylation of Runx1 at Ser249 and Ser266 or Ser249 and Ser276 is not essential for bone marrow hematopoiesis. (A) Expression patterns of the indicated surface markers in the indicated bone marrow fractions from *wild-type* (WT), *Runx1*$^{PM12A/PM12A}$ (12A) and *Runx1*$^{PM13A/PM13A}$ (13A) mice show normal differentiation of progenitor populations. (B) Normal colony-forming activity in *Runx1*$^{PM12A/PM12A}$ and *Runx1*$^{PM13A/PM13A}$ mice.

tion [16], we examined whether *Runx1*^{PM12A} or *Runx1*^{PM13A} mutation affects the differentiation of $CD4^+CD8^+$DP thymocytes. There were no significant changes detected in the number of $CD4^+CD8^+$DP thymocytes or in the percentage of $TCR\beta^{hi}HSA^{hi}$ post-selection thymocytes (Fig. 4A and B). In addition, decrease in the percentage of mature thymocytes resulting from the loss of Runx1 was not observed either in *Runx1*$^{PM12A/PM12A}$ or *Runx1*$^{PM13A/PM13A}$ mice. The ratio of $CD4^+$ single positive (SP) thymocytes to $CD8^+$ SP thymocytes in mature thymocytes ($TCR\beta^{hi}HSA^{lo}$) was slightly lower in *Runx1*$^{PM13A/PM13A}$ mutant mice, while loss of Runx1 led to a significant decrease in the number of mature CD4-lineage thymocytes [16]. Thus, putative Erk phosphorylation sites are not essential for Runx1-mediated gene regulation, which is important for positive selection and maturation of CD4-lineage thymocytes.

Runx1 is also involved in $CD4^+$ T cell homeostasis, in part by maintaining the expression of IL-7Rα [16]. Although a decrease in the number of $CD4^+$ T cells by loss of Runx1 protein were sufficient enough to reverse the ratio of $CD4^+$ T cells to $CD8^+$ T cells [16], we observed only a modest decrease in $CD4^+$ T cells in the periphery (Fig. 4C and D) and normal IL-7Rα expression levels on $CD4^+$ T cells in *Runx1*$^{PM12A/PM12A}$ and *Runx1*$^{PM13A/PM13A}$ mice (Supplementary Fig. S3)). Finally, while NKT cell development was defective in mice lacking Runx1 in thymus [20], normal NKT cell development was observed in *Runx1*$^{PM12A/PM12A}$ and *Runx1*$^{PM13A/PM13A}$ mice (Fig. 4E).

Using a combined biochemical and genetic approach, our study revealed that the Runx1 protein exists in two phosphorylated forms at least in lymphocytes. Generation of the major phosphorylated form requires the Ser249 residue, suggesting that phosphorylation on this serine residue triggers sequential phosphorylation. It is unclear which kinase(s) is involved in generation these two phosphorylated forms. Since two phosphorylated forms are detected in DN thymocytes, these phosphorylation events could occur independent of TCR engagement. However, it is still possible that Runx1 is phosphorylated by some basic Erk activity that is independent from TCR stimulation. Further studies using Erk1/Erk2 deficient thymocytes would be helpful to address this issue.

Although both *Runx1*$^{PM12A/PM12A}$ and *Runx1*$^{PM13A/PM13A}$ mice not only were devoid of phosphorylation on Ser249, Ser266, and Ser276, but also lacked major phosphorylated forms of Runx1, hematopoiesis and lymphocytes development in those mice remained normal. These observations counter findings made in previous studies involving phosphorylation-dependent trans-activation activity of Runx1 in transfection assay. The maximum trans-activation activity detectable in a transfection assay may be dependent upon the phosphorylation of Runx1. However, the latter is unlikely to be essential to minimum Runx1 activity that is sufficient for normal hematopoiesis in *Runx1*$^{PM12A/PM12A}$

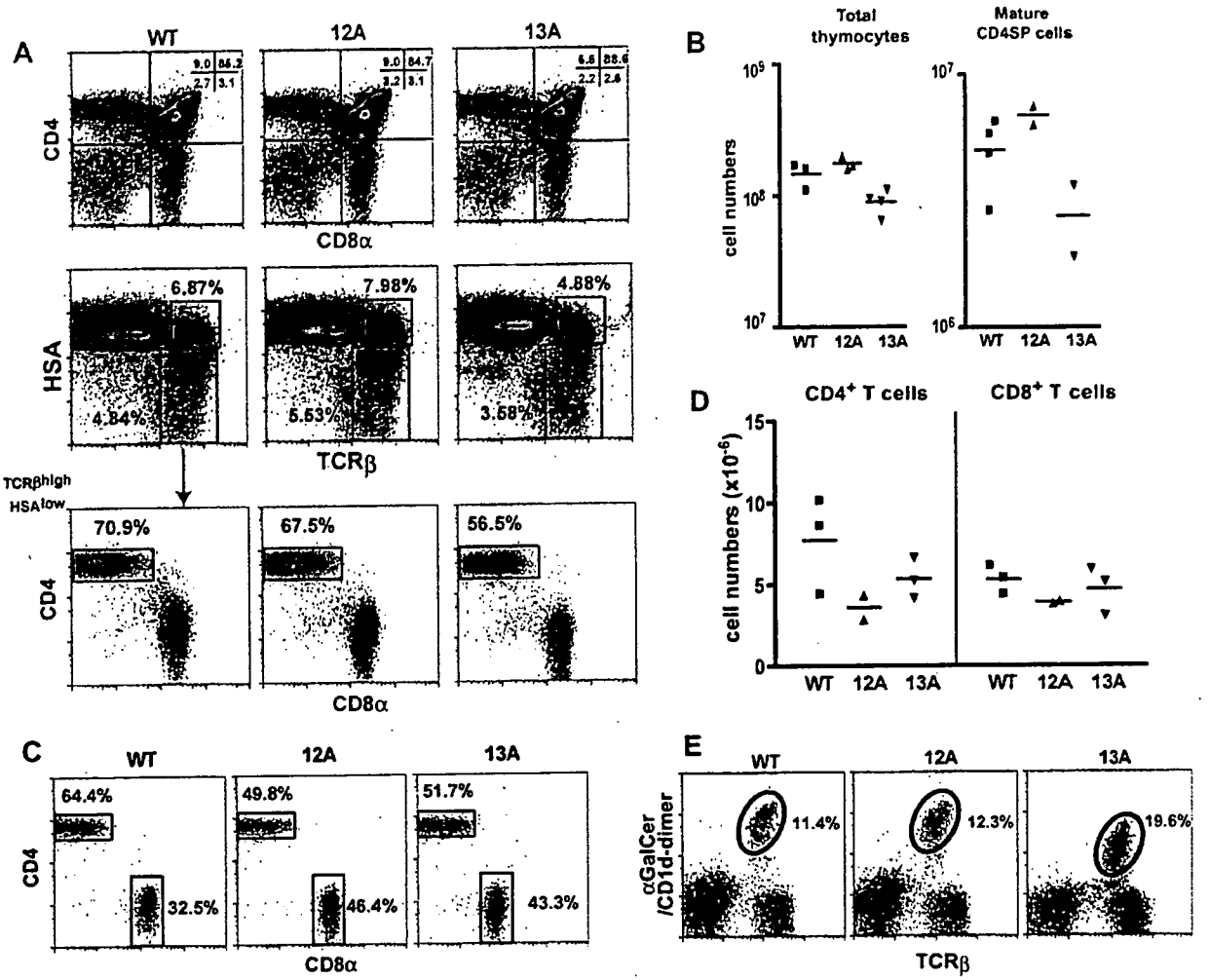

Fig. 4. Phosphorylation of Runx1 at Ser249 and Ser266 or Ser249 and Ser276 is not essential for T cell development. (A) Expression patterns of the indicated surface markers in total thymocytes or mature ($TCR\beta^{hi}HSA^{lo}$) thymocytes from *wild-type* (WT), *Runx1*$^{PM12A/PM12A}$ (12A) and *Runx1*$^{PM13A/PM13A}$ (13A) mice. (B) Cell numbers of total thymocytes and mature CD4 SP thymocytes. (C) CD4 and CD8 expression profile in $TCR\beta^{+}$ splenocytes. (D) Cell numbers of $CD4^{+}$ and $CD8^{+}$ splenic T cells from the indicated genotyped mice. (E) Normal NKT cell development in *Runx1*$^{PM12A/PM12A}$ (12A) and *Runx1*$^{PM13A/PM13A}$ (13A) mice.

and *Runx1*$^{PM13A/PM13A}$ mice. It is therefore possible that a competitive repopulation assay in host mice would reveal the masked effects of *Runx1*^{PM12A} or *Runx1*^{PM13A} mutation. Alternatively, as Runx1 and Runx3 have redundant functions each other during thymocyte differentiation [16], the effect of *Runx1*^{PM12A} and *Runx1*^{PM13A} mutations would become apparent under a Ruxn3-deficient background.

At any rate, to address the physiological relevance of post-translational modifications, gene targeting-based "knock-in" mutagenesis would likely be the most reliable approach. Our results in this study cannot rule out the possibility that phosphorylation events on unidentified residues may play important roles in regulating Runx1 function. Indeed recent studies have reported that phosphorylation of Runx1 by cyclin-dependent kinase on residues other than Ser249, Ser266, and Ser276 was important for trans-activation of Runx1 protein [21]. Further mutation-based approaches are needed to identify those residues that are involved in the key post-translational modifications of Runx1.

Acknowledgments

We thank S. Mochizuki for injecting the ES clones, and M. Taniguchi for providing the αGalCer/CD1d-dimer. This work was supported by grants from PRESTO, JST.

Appendix A. Supplementary data

Supplementary data associated with this article can be found, in the online version, at doi:10.1016/j.bbrc.2008.01.124.

References

[1] A.J. van Wijnen, G.S. Stein, J.P. Gergen, Y. Groner, S.W. Hiebert, Y. Ito, P. Liu, J.C. Neil, M. Ohki, N. Speck, Nomenclature for Runt-related (RUNX) proteins, Oncogene 23 (2004) 4209–4210.

[2] M.F. de Bruijn, N.A. Speck, Core-binding factors in hematopoiesis and immune function, Oncogene 23 (2004) 4238–4248.

[3] J. Lee, J. Ahnn, S.C. Bae, Homologs of RUNX and CBF beta/PEBP2 beta in *C. elegans*, Oncogene 23 (2004) 4346–4352.

[4] T. Komori, Runx2, a multifunctional transcription factor in skeletal development, J. Cell. Biochem. 87 (2002) 1–8.

[5] J. Canon, U. Banerjee, Runt and Lozenge function in *Drosophila* development, Semin. Cell Dev. Biol. 11 (2000) 327–336.

[6] T. Okuda, J. van Deursen, S.W. Hiebert, G. Grosveld, J.R. Downing, AML1, the target of multiple chromosomal translocations in human leukemia, is essential for normal fetal liver hematopoiesis, Cell 84 (1996) 321–330.

[7] Q. Wang, T. Stacy, M. Binder, M. Marin-Padilla, A.H. Sharpe, N.A. Speck, Disruption of the Cbfa2 gene causes necrosis and hemorrhaging in the central nervous system and blocks definitive hematopoiesis, Proc. Natl. Acad. Sci. USA 93 (1996) 3444–3449.

[8] A.T. Look, Oncogenic transcription factors in the human acute leukemias, Science 278 (1997) 1059–1064.

[9] M. Osato, N. Asou, E. Abdalla, K. Hoshino, H. Yamasaki, T. Okubo, H. Suzushima, K. Takatsuki, T. Kanno, K. Shigesada, Y. Ito, Biallelic and heterozygous point mutations in the runt domain of the AML1/PEBP2alphaB gene associated with myeloblastic leukemias, Blood 93 (1999) 1817–1824.

[10] H. Miyoshi, K. Shimizu, T. Kozu, N. Maseki, Y. Kaneko, M. Ohki, t(8;21) breakpoints on chromosome 21 in acute myeloid leukemia are clustered within a limited region of a single gene, AML1, Proc. Natl. Acad. Sci. USA 88 (1991) 10431–10434.

[11] Y. Aikawa, L.A. Nguyen, K. Isono, N. Takakura, Y. Tagata, M.L. Schmitz, H. Koseki, I. Kitabayashi, Roles of HIPK1 and HIPK2 in AML1- and p300-dependent transcription, hematopoiesis and blood vessel formation, EMBO J. 25 (2006) 3955–3965.

[12] T. Tanaka, M. Kurokawa, K. Ueki, K. Tanaka, Y. Imai, K. Mitani, K. Okazaki, N. Sagata, Y. Yazaki, Y. Shibata, T. Kadowaki, Hirai, The extracellular signal-regulated kinase pathway phosphorylates AML1, an acute myeloid leukemia gene product, and potentially regulates its transactivation ability, Mol. Cell. Biol. 16 (1996) 3967–3979.

[13] Y. Zhang, J.R. Biggs, A.S. Kraft, Phorbol ester treatment of K562 cells regulates the transcriptional activity of AML1c through phosphorylation, J. Biol. Chem. 279 (2004) 53116–53125.

[14] T.L. Aho, J. Sandholm, K.J. Peltola, Y. Ito, P.J. Koskinen, Pim-1 kinase phosphorylates RUNX family transcription factors and enhances their activity, BMC Cell. Biol. 7 (2006) 21.

[15] I. Taniuchi, M. Osato, T. Egawa, M.J. Sunshine, S.C. Bae, T. Komori, Y. Ito, D.R. Littman, Differential requirements for Runx proteins in CD4 repression and epigenetic silencing during T lymphocyte development, Cell 111 (2002) 621–633.

[16] T. Egawa, R.E. Tillman, Y. Naoe, I. Taniuchi, D.R. Littman, The role of the Runx transcription factors in thymocyte differentiation and in homeostasis of naive T cells, J. Exp. Med. 204 (2007) 1945–1957.

[17] K.J. Oestreich, R.M. Cobb, S. Pierce, J. Chen, P. Ferrier, E.M. Oltz, Regulation of TCRbeta gene assembly by a promoter/enhancer holocomplex, Immunity 24 (2006) 381–391.

[18] M. Ichikawa, T. Asai, T. Saito, S. Seo, I. Yamazaki, T. Yamagata, K. Mitani, S. Chiba, S. Ogawa, M. Kurokawa, H. Hirai, AML-1 is required for megakaryocytic maturation and lymphocytic differentiation, but not for maintenance of hematopoietic stem cells in adult hematopoiesis, Nat. Med. 10 (2004) 299–304.

[19] J. Alberola-Ila, G. Hernandez-Hoyos, The Ras/MAPK cascade and the control of positive selection, Immunol. Rev. 191 (2003) 79–96.

[20] T. Egawa, G. Eberl, I. Taniuchi, K. Benlagha, F. Geissmann, L. Hennighausen, A. Bendelac, D.R. Littman, Genetic evidence supporting selection of the Valpha14i NKT cell lineage from double-positive thymocyte precursors, Immunity 22 (2005) 705–716.

[21] L. Zhang, F.B. Fried, H. Guo, A.D. Friedman, Cyclin-dependent kinase phosphorylation of RUNX1/AML1 on three sites increases trans-activation potency and stimulates cell proliferation, Blood (2007).

The American Journal of Pathology, Vol. 171, No. 1, July 2007

DOI: 10.2353/ajpath.2007.070033

Phosphorylation of Ephrin-B1 Regulates Dissemination of Gastric Scirrhous Carcinoma

Masamitsu Tanaka,* Reiko Kamata,* Misato Takigahira,† Kazuyoshi Yanagihara,† and Ryuichi Sakai*

From the Growth Factor Division, Central Animal Laboratory,† National Cancer Center Research Institute, Tokyo, Japan*

Interaction of the Eph family of receptor protein tyrosine kinase and its ligand ephrin family induces bidirectional signaling via cell-cell contacts. High expression of B-type ephrin is frequently found in various cancer cells, and their expression levels are associated with high invasion of tumors and poor prognosis. However, whether ephrin-B1 actually promotes invasion of cancer cells *in vivo* has not been shown. We investigated the involvement of ephrin-B1 in regulating the invasiveness of scirrhous gastric cancer, which is a diffusely infiltrative carcinoma with high invasion potential. Reduction of ephrin-B1 expression by short interfering RNA or overexpression of phosphorylation-defective mutant suppressed migration and invasion of scirrhous gastric cancer cells *in vitro* without affecting tumor cell proliferation and apoptosis. Blocking of tyrosine phosphorylation of ephrin-B1 attenuates not only dissemination of cancer cells injected intraperitoneally but also local invasion and dissemination of orthotopically implanted cancer cells in the gastric wall of nude mice. Furthermore, blocking of ephrin-B1 phosphorylation attenuated the activation of Rac1 GTPase in these invasive gastric cancer cells. Our results suggest that tyrosine phosphorylation of ephrin-B1 promotes invasion of cancer cells *in vivo* and is a potential therapeutic target in some types of gastrointestinal cancers. (Am J Pathol 2007, 171:000–000; DOI: 10.2353/ajpath.2007.070033)

Members of the Eph receptor family can be classified into two groups based on their sequence similarity and their preferential binding to the subset of ligands tethered to the cell surface either by a glycosylphosphatidyl inositol-anchor (ephrin-A) or a transmembrane domain (ephrin-B).[1–3] Interaction of the EphB family of receptor protein tyrosine kinases and its ligand ephrin-B family induces bidirectional signaling via cell-cell contacts.

The biological functions of Ephs and ephrins in epithelial cells and tumors have recently been highlighted.[4–9] For example, EphB receptors and ephrin-B ligands are expressed in normal intestinal epithelium, which contributes for the restriction of cell migration and positioning along the crypt-villus axis.[4] Overexpression of B-type ephrin in cancer cells correlates with poor prognosis characterized by high invasion and high vascularity of the tumors.[10–15] Expression of ephrin-B2 has been reported in invasive tumor cells and is often highly expressed in the peripheral region of the tumors especially at the front of the invasion.[11] Ephrin-B1 is frequently overexpressed in gastrointestinal tumors, especially in poorly differentiated invasive tumor cells.[15] Although an accumulating number of reports have suggested that expression of B-type ephrin is closely associated with tumor cell invasion, whether ephrin-B modifies tumor invasion *in vivo* has not been well established.

Ephrin-Bs are tyrosine phosphorylated via Src family kinases in response to the interaction with EphB receptors, which serves as a docking site for Src homology 2 domain of adaptor protein Grb4, and transduce intracellular signaling.[16,17] We have also demonstrated that ephrin-B1 is phosphorylated independently of Eph receptors through association with an intercellular adhesion molecule, which leads to attenuation of cell-cell adhesion.[7] In our recent observations, signaling mediated by ephrin-B1 promoted the process of intracellular transport and secretion of matrix metalloproteinase (M. Tanaka, K. Sasaki, R. Kamata, and R. Sakai, unpublished data), which led us to examine in this study whether disruption of ephrin-B1-mediated signaling, especially through the tyrosine phosphorylation of ephrin-B1, could suppress tumor cell invasion.

Scirrhous gastric carcinoma diffusely infiltrates a broad region of the stomach and frequently associates with metastasis to lymph nodes and peritoneal dissemi-

Supported by the Program for the Promotion of Fundamental Studies in Health Science of the Organization for Pharmaceutical Safety and Research of Japan.

Accepted for publication April 10, 2007.

Supplemental material for this article can be found on *http://ajp.amjpathol.org*.

Address reprint requests to Ryuichi Sakai, Growth Factor Division, Central Animal Laboratory, National Cancer Center Research Institute, 5-1-1 Tsukiji, Chuo-ku, Tokyo 104-0045. E-mail: rsakai@gan2.res.ncc.go.jp.

nation and, therefore, has the worst prognosis among various types of gastric cancers. We previously established two cell lines of human gastric scirrhous carcinoma possessing high infiltrative potential by repeating cycles of orthotopic transplantation in nude mice and collecting cancer cells from the ascitic fluid formed as a result of cancerous peritonitis.[18,19] In this study, we show that reduction of ephrin-B1 expression or blocking of tyrosine phosphorylation of ephrin-B1 inhibits tumor invasion of these highly invasive gastric cancer cells. Our results suggest that ephrin-B1 represents a rational therapeutic target and that suppression of its phosphorylation is a strategy for modulating the invasion of some types of cancers.

Materials and Methods

Plasmids, Antibodies, and Reagents

Plasmids encoding full-length cDNAs of human ephrin-B1 and ephrin-B1 with mutations of four tyrosine residues in the cytoplasmic domain (Y313, 317, 324, and 329) ephrin-B1 4YF have already been described.[7] To generate the recombinant retrovirus, cDNAs were subcloned into the vector pDON-AI (Takara, Kyoto, Japan). The rabbit polyclonal antibodies for ephrin-B1 (C18) and α-tubulin were purchased from Santa Cruz Biotechnology, Inc. (Santa Cruz, CA). Polyclonal antibody against tyrosine-phosphorylated ephrin-B1 (ephrin-B1 pY317, amino acids 314 to 321, which is identical to corresponding region of ephrin-B2, 301 to 308, and ephrin-B3, 308 to 315) was raised in rabbits and affinity-purified as described previously.[7] The monoclonal antibodies for phosphotyrosine (4G10) and Rac1 were from Upstate Biotechnology (Lake Placid, NY). The polyclonal antibodies for EphB2 and EphB4 were from R&D Systems (Minneapolis, MN). Fibronectin (bovine), collagen type I, and Matrigel basement membrane matrices were purchased from Sigma (St. Louis, MO), Nitta Gelatin, Inc. (Osaka, Japan), and BD Biosciences (San Jose, CA), respectively.

Cell Culture and Transfection

Gastric carcinoma cell lines were cultured in RPMI 1640 medium supplemented with 10% fetal bovine serum. Mouse fibroblast L cells were cultured in Dulbecco's modified Eagle's medium with 10% fetal bovine serum. L cells stably expressing EphB2 (L EphB2) were established through transfection of a plasmid encoding human ephrin-B1 in parent L cells, which do not express cognate receptors for ephrin-B1 as previously described,[7] and selection in medium containing hygromycin B at a concentration of 400 μg/ml. Recombinant retroviral plasmid pDON-AI was cotransfected with pCL-10A1 retrovirus packaging vector (Imgenex, San Diego, CA) into 293gp cells to allow the production of retroviral particles. Gastric cancer cells stably expressing ephrin-B1 4YF were established by infecting cancer cells with retroviruses and selected in the medium containing G418 at a concentration of 500 μg/ml for 3 weeks. The mixture of selected cells was used for the experiments.

In Vitro *Short Interfering RNA (siRNA) Treatment*

Two sets of Stealth siRNAs of ephrin-B1 were synthesized as follows (Invitrogen, Carlsbad, CA): ephrin-B1 sense 1, 5′-UAAGGGAAUGAUGAUGUCGCUGGGC-3′; ephrin-B1 antisense 1, 5′-GCCCAGCGACAUCAUCAUUCCCUUA-3′; ephrin-B1 sense 2, UAGUCCGUAAGGGAAUGAUGAUGUC-3′; and ephrin-B1 antisense 2, GACAUCAUCAUUCCCUUACGGACUA-3′. The control siRNA (scramble II duplex, 5′-GCGCGCUUUGUAGGAUUCGdTdT-3′) was purchased from Dharmacon (Lafayette, CO). siRNAs were incorporated into cells using Lipofectamine2000 according to the manufacturer's instructions (Invitrogen). Assays were performed 72 hours after treatment.

Immunoprecipitation

Cell lysates were prepared with protease inhibitors in PLC buffer [50 mmol/L 4-(2-hydroxyethyl)-1-piperazineethanesulfonic acid, pH 7.5, 150 mmol/L NaCl, 1.5 mmol/L $MgCl_2$, 1 mmol/L ethylene glycol bis(β-aminoethyl ether)-*N,N,N′,N′*-tetraacetic acid, 10% glycerol, 100 mmol/L NaF, 1 mmol/L Na_3VO_4, and 1% Triton X-100]. To precipitate the proteins, 1 μg of affinity-purified polyclonal antibody was incubated with 500 μg of cell lysate for 2 hours at 4°C and then precipitated with protein G agarose for 1 hour at 4°C. Immunoprecipitates were extensively washed with PLC buffer, separated by sodium dodecyl sulfate-polyacrylamide gel electrophoresis, and immunoblotted.

Affinity Precipitation

Affinity precipitation with GST-PBD (p21-binding domain of p21-activated kinase 1) was performed as described previously.[20] In brief, cells were lysed in the lysis buffer [50 mmol/L 4-(2-hydroxyethyl)-1-piperazineethanesulfonic acid, pH 7.5, 150 mmol/L NaCl, 10 mmol/L $MgCl_2$, 1 mmol/L ethylene glycol bis(β-aminoethyl ether)-*N,N,N′,N′*-tetraacetic acid, 10% glycerol, 100 mmol/L NaF, 1 mmol/L Na_3VO_4, and 1% Triton X-100] and incubated with GST-PBD on Sepharose for 1 hour at 4°C. Precipitants were washed three times in the same buffer, and endogenous Rac1 was detected by immunoblotting with anti-Rac1 antibody.

5-Bromo-2′-Deoxyuridine Incorporation

Cell proliferation was assessed by measurement of 5-bromo-2′-deoxyuridine (BrdU) incorporation into the DNA with Cell Proliferation enzyme-linked immunosorbent assay, BrdU (colorimetric) kit (Roche, Basel, Switzerland). In brief, gastric cancer cells were plated onto 96-well plates (1×10^4 cells/well) 48 hours after treatment of siRNAs and further incubated for 24 hours before the addition of BrdU. Cells were reincubated for 6 hours,

and incorporated BrdU was detected with peroxidase-labeled anti-BrdU antibody and developed with tetramethyl-benzidine as a chromogenic substrate according to the manufacturer's instructions (Roche). The absorbance of the samples was measured at the wavelength of 450 nm using a microplate reader (model 550; Bio-Rad, Hercules, CA).

Apoptosis Assays

Gastric cancer cells were plated in triplicate onto 96-well plates (1 × 10^4 cells) 48 hours after treatment of siRNAs and incubated for 24 hours. Cells were lysed to detect apoptosis by measurement of nucleosomes in the cytoplasm of apoptotic cells using a Cell Death enzyme-linked immunosorbent assay kit according to the manufacturer's instructions (Roche Molecular Biochemicals). In brief, nucleosomes in cell lysates were detected with peroxidase-labeled anti-DNA antibody and developed with 2,2′-azino-di[3-ethylbenzthiazolin-sulfonate] as a chromogenic substrate. The absorbance of the samples was measured at the wavelength of 405 nm using a microplate reader (model 550; Bio-Rad).

Cell Attachment Assay

Cancer cells were detached by phosphate-buffered saline(−) [PBS$^{(-)}$] containing ethylenediamine tetraacetic acid (2 mmol/L) and replated on the chamber slides coated with either collagen type I (100 μg/ml; Nitta Gelatin, Inc.), fibronectin (50 μg/ml; Sigma), or Matrigel (85 μg/ml; Asahi Techno Glass Co., Tokyo, Japan). After incubation for 30 minutes, unattached cells were removed by washing the slides in PBS$^{(-)}$ several times, and the remaining cells were stained with Giemsa's solution. The number of attached cells on each substrate was counted.

Cell Staining

Cells were fixed for 5 minutes at room temperature with 4% paraformaldehyde in PBS and permeabilized for 10 minutes with 0.2% Triton X-100. The cells were preincubated in 2% bovine serum albumin for 0.5 hour and incubated with Alexa546-conjugated phalloidin (Molecular Probes, Eugene, OR) for 1 hour at room temperature. Photos were taken with a Radiance 2100 confocal microscope (Bio-Rad).

Overlay Tumor Invasion Assay

Invasion of tumor cells into the monolayer of stromal cells was monitored basically as described previously.[20] Gastric cancer cells treated with ephrin-B1 siRNA or control siRNA were labeled with 2 mmol/L lipophilic tracer DiO (Molecular Probes) and then detached with Hanks' balanced salt solution$^-$ containing 2 mmol/L ethylenediamine tetraacetic acid and seeded on the confluent monolayer of parent L cells or L EphB2 cells. After being cultured in the medium with 10% fetal bovine serum for 15 hours, the cells were fixed with 4% paraformaldehyde in PBS, and the number of invasion foci of cancer cells was counted using fluorescence microscopy.

In Vivo Tumor Cell Invasion Assay

The animal experimental protocols were approved by the Committee for Ethics of Animal Experimentation, and the experiments were conducted in accordance with the guidelines for Animal Experiments in the National Cancer Center. Peritoneal dissemination of tumors was examined by intraperitoneal injection of 5 × 10^6 gastric cancer cells suspended in 0.3 ml of RPMI 1640 medium into 6-week-old BALB/c nude mice (CLEA Japan, Inc., Tokyo, Japan). The mice were sacrificed 2 weeks after injection, and peritoneal dissemination was evaluated. Orthotopic implantation of gastric cancer cells into BALB/c nude mice has been described previously.[18,19] In brief, 1 × 10^6 cells were inoculated into the middle wall of the greater curvature of the glandular stomach by using a 30-gauge needle. The mice were sacrificed at different time points after the orthotopic transplantation of the cancer cells and subjected to macroscopic and histopathological examination of the tumors.

Results

Reduction of Ephrin-B1 Expression Attenuates Tumor Invasion of Gastric Cancer Cells

To examine the involvement of ephrin-B1 for invasion of tumors, we analyzed cell lines of scirrhous gastric carcinoma, which is characterized as reduced cell-cell adhesion with high invasion potential. HSC-44PE and HSC-58 were originally established from the patients of scirrhous gastric carcinoma, and highly invasive sublines were further selected from these parent cells (44As3 from HSC-44PE; 58As1 and 58As9 from HSC-58[18,19]). Both expression and phosphorylation levels of ephrin-B1 were higher in cells of invasive sublines than in corresponding parent cell lines, whereas the expression level of control α-tubulin was not altered in these cell lines (Figure 1a). In addition, EphB2 was expressed in all of these cell lines, and HSC-44PE and 44As3 cells also expressed EphB4, showing the existence of cognate receptors (Figure 1a).

We next examined whether reduction of ephrin-B1 expression affects cell motility and proliferation of these gastric cancer cells. The treatment of cells with two independent siRNA of ephrin-B1 effectively reduced ephrin-B1 expression level in 58As9 cells and 44As3 cells (Figure 1b). In addition, phosphorylation of B class ephrin was greatly reduced by knocking down ephrin-B1, as judged by the antibody recognizing phosphorylation of all three members of ephrin-Bs at the tyrosine in the cytoplasmic region (Figure 1b). From the analysis of *in vitro* Transwell assay, reducing the amount of ephrin-B1 in 44As3 cells inhibited migration and invasion through the extracellular matrix (Figure 2a). Similar results were also observed in 58As9 cells (Figure 2a). On the other

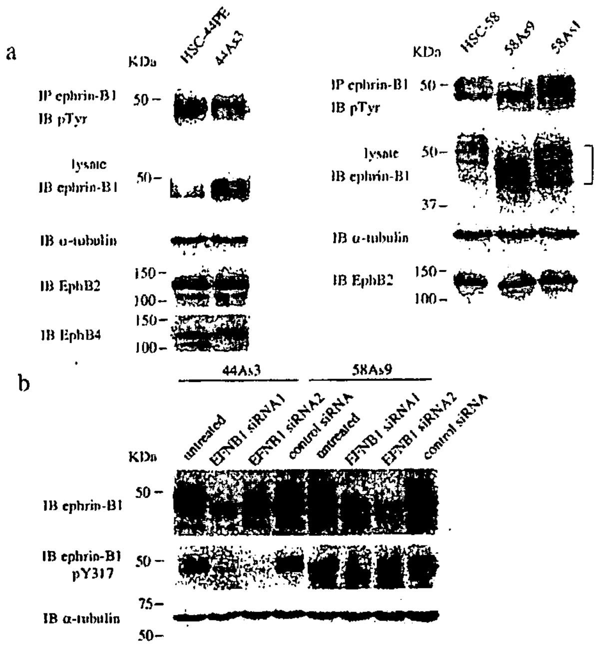

Figure 1. Tyrosine phosphorylation of ephrin-B1 is higher in invasive gastric cancer cell lines. **a:** As indicated, lysates from cells were subjected to immunoprecipitation (IP) with anti-ephrin-B1 antibody and immunoblotting (IB) with anti-phosphotyrosine antibody. The expression levels of ephrin-B1, α-tubulin, EphB2, and EphB4 in each cell lysate were confirmed by immunoblotting (bottom). When cell lysates were blotted with ephrin-B1 antibody, several ephrin-B1-reactive bands (blanket) were detected because of the glycosylation and difference in tyrosine phosphorylation as reported.[31] **b:** Cellular levels of ephrin-B1 were analyzed 72 hours after treatment with siRNAs by Western blotting using α-tubulin as a loading control. Expression of ephrin-B1 was reduced in cells treated with ephrin-B1 siRNA (EFNB1siRNA1, 2). The phosphorylation level of ephrin-Bs was assessed by the antibody recognizing phosphorylation of Tyr317 of ephrin-B1, which also detects phosphorylation of corresponding tyrosine of ephrin-B2 (Tyr304) and ephrin-B3 (Tyr311) as described in Materials and Methods.

hand, proliferation and apoptosis of these cells were not significantly affected (Figure 2b). In addition, reduction of ephrin-B1 expression did not cause remarkable change in the adhesion of 44As3 and 58As9 cells on different extracellular matrices, including type I collagen, fibronectin, and Matrigel (Figure 2c). We further examined whether overexpression of ephrin-B1 is sufficient to promote the migration and invasion of cancer cells by stably expressing ephrin-B1 in one parental cell line HSC-58. The migration and invasion through extracellular matrix was apparently increased by the overexpression of ephrin-B1 (Figure 2d).

Phosphorylation of Ephrin-B1 Promotes Migration and Invasion of Gastric Cancer Cells

Because the level of tyrosine phosphorylation of ephrin-B1 was higher in invasive sublines of gastric cancer cells, we next examined whether blocking of ephrin-B1 phosphorylation in these cells attenuates their migration and invasion. The stable expression of ephrin-B1 with mutations of four tyrosine residues in the cytoplasmic domain (Y313, 317, 324, and 329) ephrin-B1 4YF reduced the tyrosine phosphorylation level of ephrin-B1 in 44As3 and 58As9 cells, because overexpression of ephrin-B1 4YF prevents endogenous ephrin-B1 from association with EphB receptors expressed in these cells (Figure 3a). From the analysis of *in vitro* Transwell assay, migration and invasion of cancer cells stably expressing ephrin-B1 4YF mutant (44As3 4YF and 58As9 4YF cells) were decreased compared with the control cells expressing mock vector (44As3 mock and 58As9 mock cells) (Figure 3b). On the other hand, expression of ephrin-B1 4YF did not affect cell proliferation under usual two-dimensional cell culture condition (Figure 3c). When these cancer cells expressing mock vector or ephrin-B1 4YF were implanted subcutaneously in nude mice, the mean size and weight of the tumors were not significantly different (Figure 3d). To understand the mechanism by which ephrin-B1 4YF attenuates the cell migration, we examined activity of Rac1 GTPase, which is a critical molecule controlling the organization of actin cytoskeleton. The activation of Rac1 was examined by affinity precipitation of GTP-bound Rac1 with the GST-fusion protein of the p21-binding domain of p21-activated kinase 1.[21] The activated Rac1 was apparently reduced in 44As3 or 58s9 cells expressing ephrin-B1 4YF compared with the cells expressing mock vector (Figure 3e). When the appearance of cytoskeleton of these cancer cells was examined, formation of large lamellipodia was observed in most of the mock-containing 44As3 and 58As9 cells, whereas it was less frequently observed in 44As3 4YF and 58As9 4YF cells (Figure 3f), which may be consistent with the reduced Rac1 activity in cancer cells expressing ephrin-B1 4YF.

Gastric scirrhous carcinoma frequently associates with peritoneal dissemination through the process that cancer cells perforate gastric serosa and become exfoliated and free and then attached on the surface of the peritoneum and start to invade there. The effect of ephrin-B1 expression on tumor invasion was further monitored *in vitro* by overlay tumor cell invasion assay as a model system for stromal invasion of cancer cells. When 44As3 cells were plated onto the monolayer of fibroblasts, L cells, the formation of tumor cell islands was observed as tumor cells invaded and grew between the fibroblasts (Figure 4a). The formation of such tumor islands is the sign of penetration of tumor cells into the sheet of stromal cells, as used for the evaluation of cancer cell invasion through endothelial cells or mesothelial cells.[20,22,23] The invasion of 44As3 cells into the fibroblasts monolayer was more evident when the cancer cells were plated onto L cells stably expressing EphB2 (L EphB2) than on the parent L cells, which do not express receptors for ephrin-B1[7] (Figure 4b). The invasion foci of 44As3 in monolayer of L EphB2 cells were decreased in number and size when expression of ephrin-B1 in cancer cells was reduced (Figure 4a). In addition, the invasion of 44As3 4YF cells into the monolayer of L EphB2 cells was also decreased compared with 44As3 mock cells (Figure 4, a and b). These results indicate that activation of the signaling mediated by ephrin-B1 phosphorylation in cancer cells induced by the interaction with EphB2 receptor expressed in stromal cells enhanced the tumor invasion.

The effect of ephrin-B1 phosphorylation on tumor invasion was further examined *in vivo* using 44As3 and 58As9

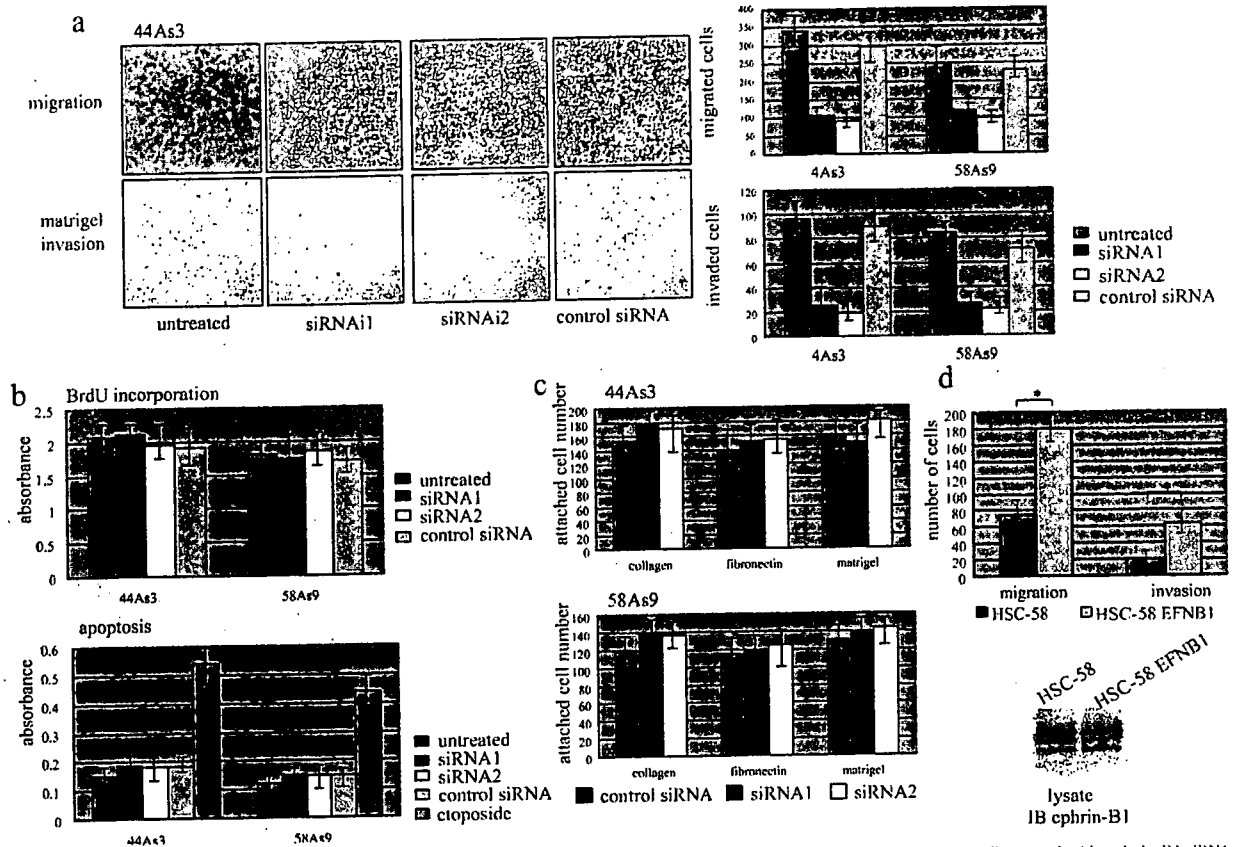

Figure 2. Reduction of ephrin-B1 expression suppressed cell motility and invasion in 44As3 and 58As9 cells. **a:** 44As3 and 58As9 cells treated with ephrin-B1 siRNA (siRNA1, 2) or control siRNA or left untreated were plated onto a Transwell membrane coated with Matrigel (bottom; 85 $\mu g/cm^2$) or uncoated (top) in serum-free medium. In the lower chamber, medium containing 5% fetal bovine serum was added as a chemoattractant. After 10 hours of incubation, the wells were harvested, and cells that migrated to the lower surface of the membrane were counted. Representative fields of 44As3 cells are shown. The results from three independent experiments, each in duplicate, are shown at the right as mean ± SD. The **asterisks** indicate differences from the cells treated with control siRNA. $^*P < 0.01$. **b:** Proliferation and apoptosis of cells were evaluated 72 hours after treatment of siRNAs. Top: Proliferation of the cells was evaluated by measurement of DNA synthesis through detection of BrdU incorporation by enzyme-linked immunosorbent assay (Roche). Bottom: Apoptosis of the cells was examined by measurement of nucleosomes through Cell death detection enzyme-linked immunosorbent assay kit (Roche). As a control, cells were treated with 50 μmol/L etoposide for 12 hours. The results from three independent experiments, each in duplicate, are shown as the mean ± SD. **c:** Reduction of ephrin-B1 expression did not significantly affect the cell adhesion to the extracellular matrix. 44As3 and 58As9 cells treated with ephrin-B1 siRNA (siRNA1, 2) or control siRNA were detached by ethylenediamine tetraacetic acid and replated on the chamber slides coated with collagen type I (100 μg/ml), fibronectin (50 μg/ml), or Matrigel (85 μg/ml). After incubation for 30 minutes, unattached cells were removed by washing the slides in PBS(−) several times, and the remaining cells were stained with Giemsa's solution. The number of attached cells on each substrate was counted, and the results from three independent experiments, each in duplicate, are shown as the mean ± SD. **d:** Expression of wild-type ephrin-B1 promotes migration and invasion of HSC-58 cells. Wild-type ephrin-B1 was stably expressed in HSC-58 cells by retrovirus-mediated gene transfer (HSC-58 EFNB1). The cells indicated were plated onto a Transwell membrane coated with Matrigel (invasion) or uncoated (migration) in serum-free medium and assayed as described in **a**. The results from three independent experiments, each in duplicate, are shown as mean ± SD. $^*P < 0.01$.

cells as a model system for peritoneal dissemination. When 58As9 or 44As3 cells expressing mock vector were injected intraperitoneally into nude mice, severe carcinomatous peritonitis was observed, as previously described (Figure 5a, top).[19] Innumerable whitish nodules were observed in the mesentery of almost all mice injected with 58As9 mock cells (Figure 5a, top left) and 44As3 mock cells (data not shown). In addition, many tumor nodules of 44As3 mock cells were observed in the peritoneal cavity, including the rectouterine region with invasion into the retroperitoneum (Figure 5a, top right). On the other hand, dissemination of cancer cells expressing ephrin-B1 4YF was apparently modest. Tumor nodules of 58As9 4YF cells in the mesentery were small in size and number compared with those of control 58As9 mock cells (Figure 5b; Table 1). Such reduction of tumor nodules in the mesentery was also observed in 44As3 cells expressing ephrin-B1 4YF (Table 1). In addition, the tumor volume involving the rectouterine region was reduced in the mice injected with 44As3 4YF cells (Figure 5c). These results suggest that ephrin-B1 promotes peritoneal dissemination of 58As9 and 44As3 gastric cancer cells through signaling mediated by its tyrosine phosphorylation.

Blocking of Tyrosine Phosphorylation of Ephrin-B1 Attenuates Tumor Invasion of Orthotopic Implanted Gastric Carcinoma

To further evaluate the effect of ephrin-B1 on the process of tumor invasion, we implanted gastric cancer cells orthotopically in the gastric submucosa of nude mice. At 15 days after implantation, 70% of 44As3 tumors expressing

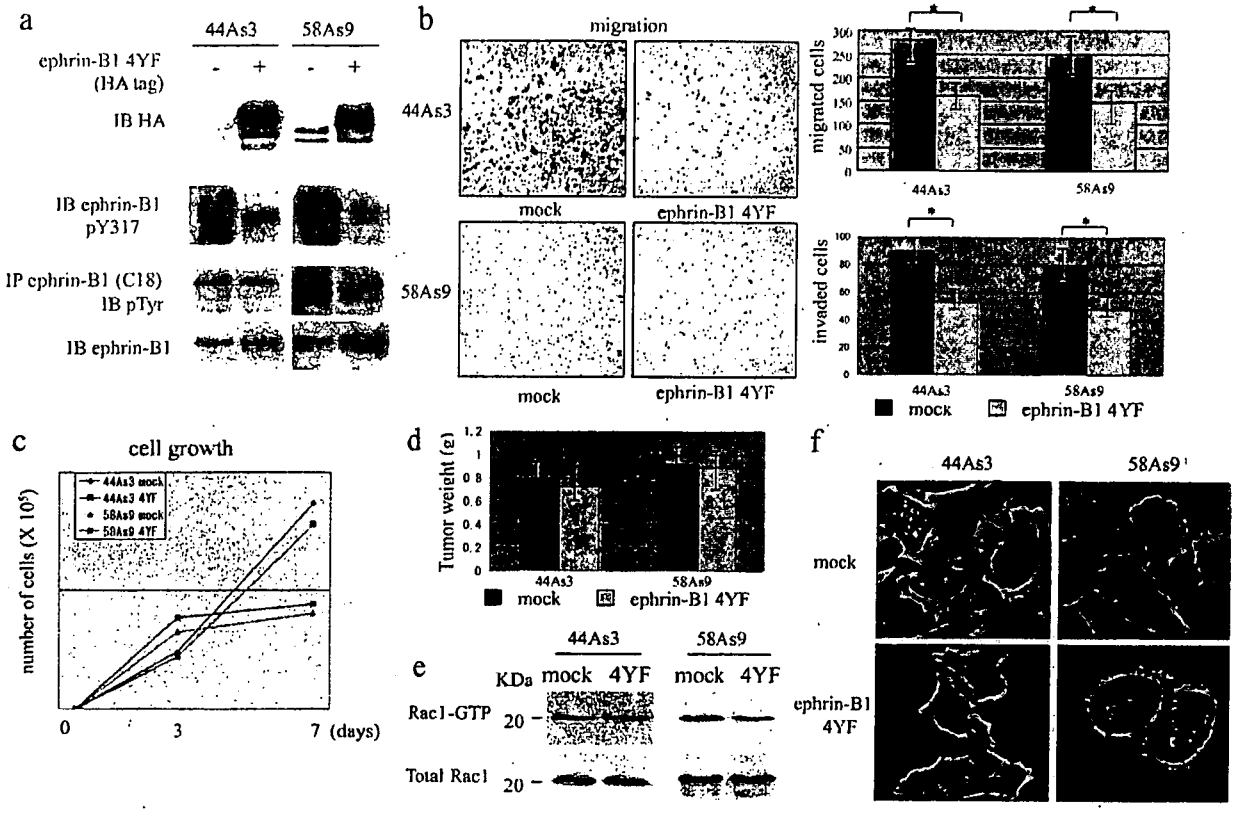

Figure 3. Blocking of ephrin-B1 phosphorylation suppressed cell migration *in vitro*. **a:** Lysates of cells stably expressing ephrin-B1 4YF tagged with HA at carboxyl terminus (+) or control mock vector (−) were subjected to immunoblotting with anti-HA antibody or tyrosine-phosphorylated ephrin-Bs (ephrin-B1 pY317) or immunoprecipitation of total ephrin-B1 and immunoblotting with anti-phosphotyrosine antibody (pTyr). The amount of immunoprecipitated ephrin-B1, which includes both endogenous ephrin-B1 and transfected ephrin-B1 4YF, is shown at the bottom. **b:** As indicated, the cells were seeded onto a Transwell membrane coated with Matrigel (invasion) or uncoated (migration) in serum-free medium as in Figure 2a. In the lower chamber, medium containing 5% fetal bovine serum was added. After 10 hours of incubation, the wells were harvested, and cells that migrated to the lower surface of the membrane were counted. Representative fields are shown. The results from three independent experiments, each in duplicate, are shown at the bottom as mean ± SD. $^{*}P < 0.01$. **c:** Proliferation of the cells under the culture in the medium containing 10% serum was evaluated by counting the cell number at different time points after being plated onto dishes. **d:** 44As3 and 58As9 cells (1×10^{7} cells/mice) expressing either mock or ephrin-B1 4YF were implanted subcutaneously in the flank of nude mice, and the mice were sacrificed 5 weeks after implantation. The mean weight ± SD of eight subcutaneous tumors is shown. **e:** Activation of Rac1 was examined by affinity precipitation of GTP-bound Rac1 (Rac1-GTP) with GST-PBD as described in Materials and Methods. The precipitated Rac1-GTP and total Rac1 in each cell lysate were detected by immunoblotting with anti-Rac1 antibody. **f:** Morphology of gastric cancer cells was monitored. The cells were fixed around 12 hours after plating and stained with phalloidin as described in Materials and Methods for detection of F-actin.

the mock vector formed a large tumor mass involving the greater omentum because of the disruption of gastric serosa and invasion into the surrounding fat tissue (Figure 6a). On the other hand, such local invasion into the omentum was less frequently observed (18%) in mice implanted with 44As3 4YF cells, and most tumors remained within the gastric wall at day 15 (Figure 6a; Table 2). The dissemination of 44As3 mock cells was also observed in several tissues, including the liver surface and mesenteric sheets (Figure 6, b and c). However, we rarely observed cancer dissemination in the peritoneal cavity in mice implanted with 44As3 4YF cells (Figure 6, b and c; Table 2).

Histological examination revealed that expression of ephrin-B1 4YF did not greatly change the morphology of the tumor in the gastric wall (Figure 7, c, d, l, and m). However, invasion of control 44As3 mock cells into lymphatic vessels in subserosa and metastasis to the regional lymph nodes was more frequently observed than 44As3 4YF cells at day 10 after tumor implantation (70 and 18%, respectively; Figure 7, e–g; Table 3). Histological analysis also revealed that the tumor had already reached the outside of the serosal surface and invaded into the surrounding fat tissue in 80% of mice implanted with 44As3 mock cells, whereas it was of low frequency in mice implanted with 44As3 4YF cells (27%) (Figure 7, h and i; Table 3). These phenotypes, including lymphatic vessel invasion, lymph node metastasis, and perforation of gastric serosa, were developed in the same mice, and all three phenotypes are overlapped in 7 of 10 mice in the mock group and in 2 of 10 mice in the 4YF group, suggesting that these are sequential or correlated events. These results indicate that the disruption of signaling mediated by phosphorylation of ephrin-B1 suppressed the invasion and peritoneal dissemination of scirrhous gastric carcinomas.

Discussion

Ephrin-B1 plays pivotal roles in the migration and invasion of cancer cells. High invasion potential is one of the

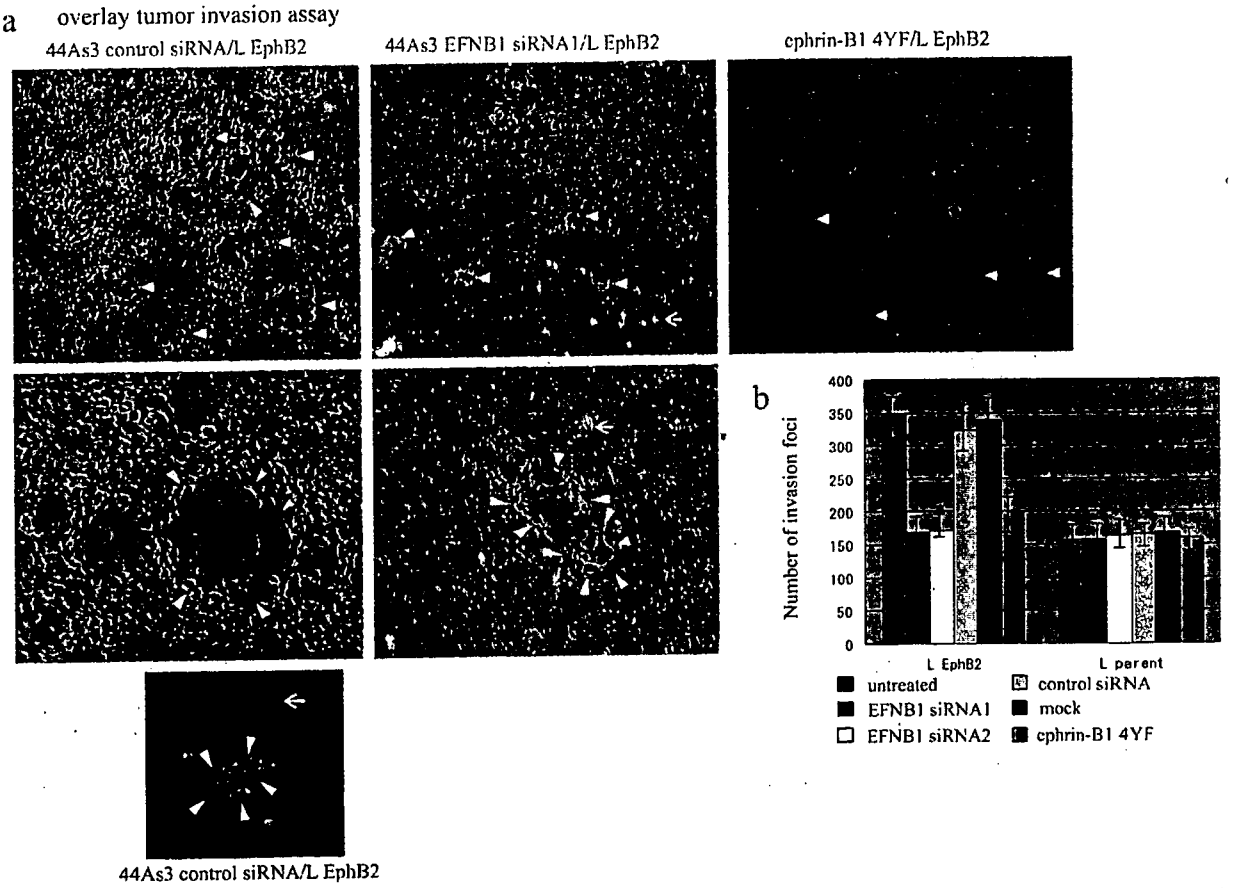

Figure 4. Invasion of ephrin-B1-expressing cells was promoted by interaction with EphB2 receptor. **a:** 44As3 cells were highly invasive into the monolayer of fibroblasts expressing EphB2, which was attenuated by reduction of ephrin-B1 expression. When L cells or L EphB2 cells grew to confluent state in 24-well plates, DiO-labeled 44As3 cells treated either with control or ephrin-B1 siRNA or with 44As3 mock or 44As3 4YF cells (1×10^5, each) were seeded onto the monolayer and incubated in a medium containing 10% fetal bovine serum for 15 hours. Representative fields of the co-culture are shown (top, ×100; bottom, ×200). **Arrowheads** indicate typical invasion foci of tumor cells. Bottom: Typical invasion focus of tumor cells is shown in the fluorescence field (×200). The nest of invaded tumor cells is surrounded by **arrowheads**. **b:** The number of invasion foci was counted as described in Materials and Methods, and the results from three independent experiments, each in duplicate, are shown as mean ± SD. The **asterisks** indicate differences from the cells treated with control siRNA or control cells expressing mock vector. $^*P < 0.01$. The **arrows** indicate unfocused DiO-labeled tumor cells, which did not invade but grew on the monolayer.

major characteristics of scirrhous carcinoma, which determines the poor prognosis of this type of cancer. Using two scirrhous gastric cancer cell lines with high invasion potential, we show for the first time that ephrin-B1 modifies cancer invasion *in vivo*. Blocking of the signaling mediated by tyrosine phosphorylation of ephrin-B1 suppressed the invasion and peritoneal dissemination of these scirrhous cancer cells. Notably, attenuation of phosphorylation of ephrin-B1 suppressed orthotopically implanted scirrhous cancer cells invading through the gastric wall and into the lymphatic vessels. The significance of ephrin-B1 in the invasive phenotype of cancer cells was further obtained from the result that stable expression of wild-type ephrin-B1 in HSC-58, the parental cell line of 58As9 cells, actually promoted the migration and invasion of this cell line *in vitro* (Figure 2d).

Association with EphB receptors triggers tyrosine phosphorylation of ephrin-B1, including Tyr317 (corresponding to Tyr298 of *Xenopus* ephrin-B1), by Src family kinases, which is a critical requirement for interaction with an Src homology 2/Src homology 3 adaptor, Grb4, to transduce signaling.[16] In the physiological conditions, phosphorylation of ephrin-B1 is induced by the contact of ephrin-B1-expressing cells with heterologous cells expressing EphB receptors. On the other hand, ephrin-B1 also promotes migration of cancer cells in a cell-autonomous mechanism as observed in Transwell assay (Figures 2 and 4b). Because EphB2 receptor was expressed in 44As3 and 58As9 cells and expression of EphB4 was also detected in 44As3 cells (Figure 1a), there is a possibility that ephrin-B1 in these cancer cells may be constitutively stimulated by EphB receptors coexpressed in the same cell surface or contacting neighboring cancer cells. This conclusion may be consistent with the observation that the basal phosphorylation level of ephrin-B1 is elevated in 44As3 and 58As9 cells under the usual two-dimensional culture condition *in vitro* (Figure 1a). Overexpression of ephrin-B1 4YF may suppress tumor invasion *in vivo* by blocking cell autonomous phosphorylation of ephrin-B1 in cancer cells and the induction of ephrin-B1 phosphorylation through the interaction with stromal cells. There is still the possibility that expression of eph-

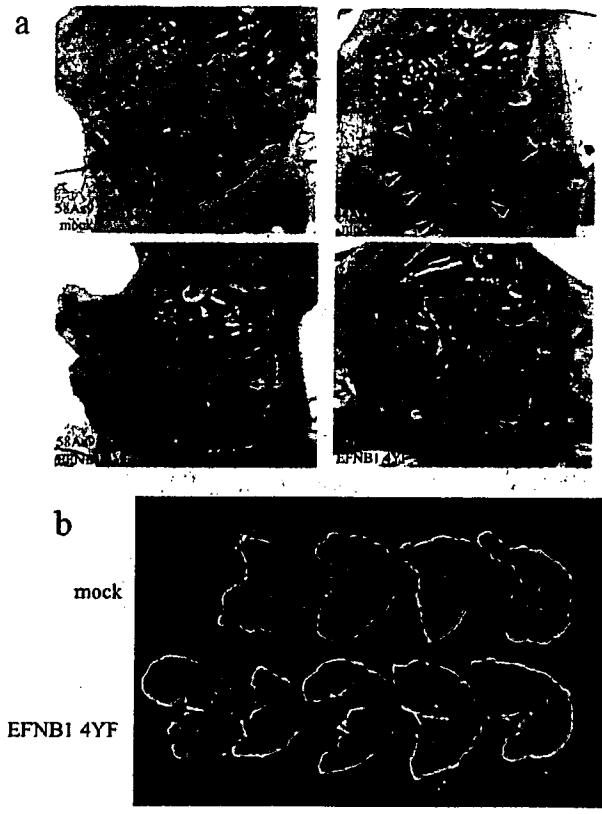

Figure 5. Disruption of ephrin-B1 phosphorylation suppressed the peritoneal dissemination of 44As3 and 58As9 cells. Cells stably expressing a mock vector or ephrin-B1 4YF were injected intraperitoneally into nude mice (5×10^6 cells/mice). **a:** Representative appearance of peritoneal dissemination two weeks after injection is shown. Left: **Asterisk** indicates dissemination of cancer nodules in the mesentery, and **arrows** indicate the tumor mass, including greater omentum. Right: The pictures were taken after resection of intestinal loops. **Arrowheads** indicate the tumor nodules of 44As3 cells disseminated around the rectouterine region and retroperitoneum. **b:** Representative dissected intestinal loops from four or five mice injected with 58As9 mock or 58As9 4YF cells, respectively. Note large tumor nodules in the mesentery of mice injected with control mock cells. **c:** Representative appearance of the tumors of 44As3 cells involving rectouterine region was compared. **Yellow** and **red arrowheads** indicate uterine horns and tumor mass, respectively.

rin-B1 4YF may also block the signaling mediated by other members of ephrin-Bs that also bind the similar group of EphB receptors. However, knocking down of ephrin-B1 by siRNA greatly reduced the phosphorylation of total ephrin-Bs (Figure 1b), suggesting that ephrin-B1, but not ephrin-B2 or ephrin-B3, is the major member of B-class ephrin, which is phosphorylated in these cells. Consistent with this conclusion, at least treatment of 44As3 and 58As9 cells with ephrin-B2 siRNA did not affect the phosphorylation level of the corresponding tyrosine residue of ephrin-Bs examined by anti-ephrin-B1 pY317 antibody (data not shown).

The ephrin/Eph interaction provides both ephrin-B1-mediated reverse signaling and EphB-mediated forward signaling. The expression of ephrin-B1 4YF may suppress the invasion of gastric cancer cells by stimulation of EphB receptor-mediated forward signaling in cancer cells through acting as a stimulator of EphB receptors, because EphB receptor-mediated forward signaling inhibited migration of colorectal tumors in a recent report.[24] However, cancer cell invasion was also inhibited by treatment with ephrin-B1 siRNA, which should cause reduction of forward signaling. Therefore, such inhibitory effect of forward signaling caused by the overexpression of the ligand, even if it exists, does not seem to be strong. In addition, we previously observed that overexpression of ephrin-B1 in Panc1 and Capan1 pancreas cancer cells, in which EphB2 is endogenously expressed, promoted the peritoneal dissemination of these cells by the similar experiment in this study (data not shown), which may also support this conclusion.

We observed that ephrin-B1-expressing cancer cells invaded more frequently into the monolayer of fibroblasts expressing EphB2 receptor than into the parent fibroblasts in overlay invasion assay. This result suggests that cancer cells expressing ephrin-B1 may actively invade into the stromal tissues that express EphB receptors, and such mechanism may also be involved in the process of peritoneal dissemination of ephrin-B1-expressing cancer cells *in vivo*. For example, stromal cells composed of mouse mesentery sheets actually expressed cognate receptors for ephrin-B1 (Supplemental Figure 1 at *http://ajp.amjpathol.org*). Again, there is a possibility that EphB2-mediated forward signaling in L EphB2 fibroblasts also contributes to the formation of invasion foci of cancer cells in this overlay assay. However, expression of ephrin-B1 4YF prevented the invasion of 44As3 cells into the monolayer of L EphB2 cells, suggesting that this invasion

Table 1. Mesenterial Dissemination after Intraperitoneal Inoculation of Gastric Cancer Cells

Cell	Number of nodules*		
	0 to 10	10 to 30	>30
44As3 mock	0	5	15
44As3 4YF	14	5	1
58As9 mock	0	2	18
58As9 4YF	16	3	1

Mice were sacrificed at 14 days after inoculation. Data are shown as the number of mice bearing tumors in the mesentery.
*Number of tumor nodules larger than 2 mm in the mesentery.

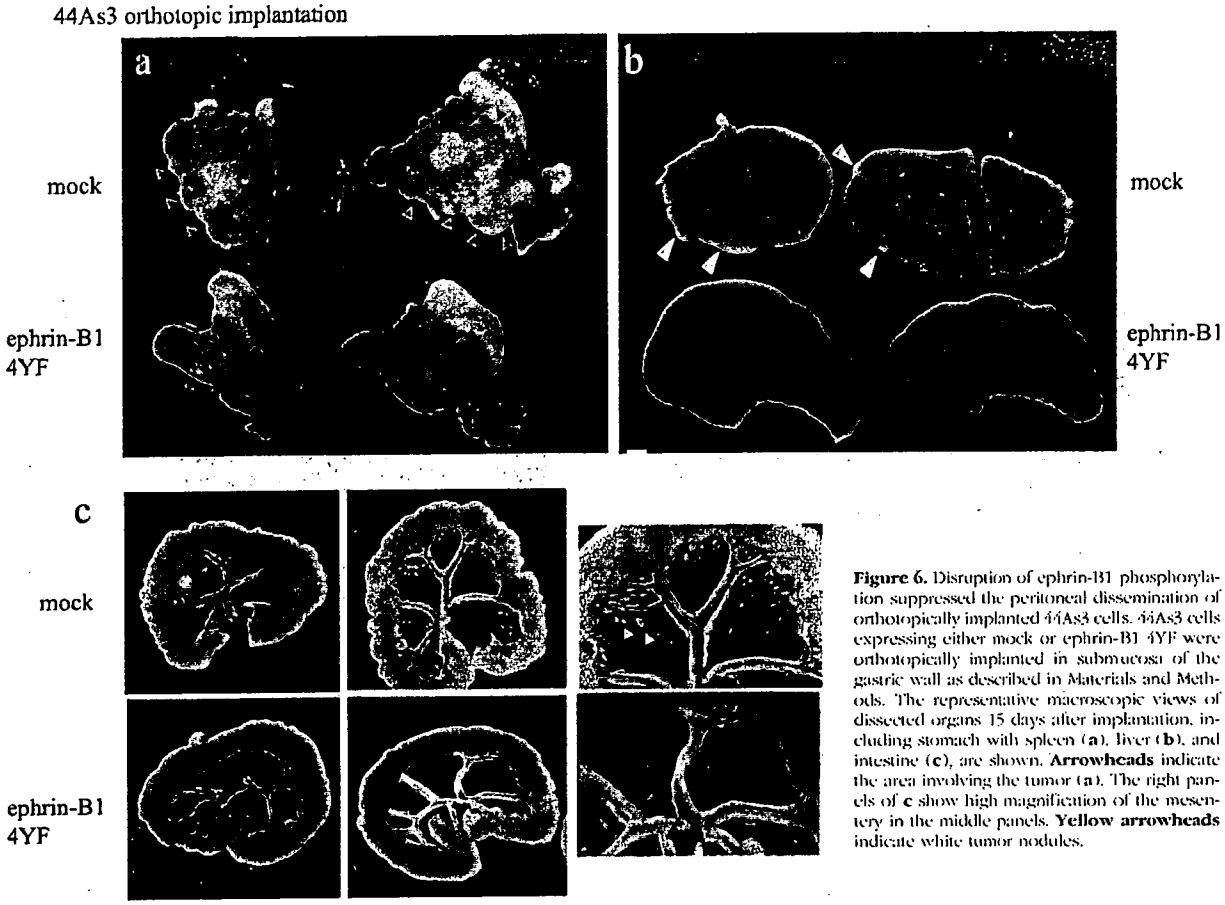

Figure 6. Disruption of ephrin-B1 phosphorylation suppressed the peritoneal dissemination of orthotopically implanted 44As3 cells. 44As3 cells expressing either mock or ephrin-B1 4YF were orthotopically implanted in submucosa of the gastric wall as described in Materials and Methods. The representative macroscopic views of dissected organs 15 days after implantation, including stomach with spleen (**a**), liver (**b**), and intestine (**c**), are shown. **Arrowheads** indicate the area involving the tumor (**a**). The right panels of **c** show high magnification of the mesentery in the middle panels. **Yellow arrowheads** indicate white tumor nodules.

is considered to depend predominantly on the ephrin-B1-mediated reverse signaling in cancer cells rather than the forward signaling in fibroblasts.

Tumor cells expressing ephrin-B1 may gain invasiveness in multiple steps of the cell invasion process. Phosphorylation of ephrin-B1 leads to the recruitment of scaffolding protein disheveled via Grb4, which results in aberrant activation of RhoA.[25,26] Ephrin-B1 makes a complex with Tiam1 to induce Rac1 activation,[20] and we showed blocking of tyrosine phosphorylation of ephrin-B1 decreased the Rac1 activity in this study. Ephrin-B1 is also phosphorylated on tyrosine residues through physical association with cell adhesion proteins such as claudin, which attenuates the cell-cell adhesion.[7] In addition, EphB2-induced phosphorylation of ephrin-B1 has been reported to modify the cell-to-substrate adhesion,[17] although reduction of ephrin-B1 with siRNA did not significantly affect cell adhesion to several substrates *in vitro* under the condition that ephrin-B1 was not stimulated with exogenous EphB2 receptor. Therefore, phosphorylation of ephrin-B1 may regulate cell motility also by affecting the cell adhesion to substrates in the process of stromal invasion of tumors *in vivo*. Blocking of ephrin-B1 phosphorylation by the ephrin-B1 4YF mutant may inhibit tumor invasion through blocking such multiple events.

We cannot exclude a possibility that phosphorylation-independent signaling of ephrin-B1 is also involved in the regulation of cancer cell invasion. For example, proteins containing PDZ domains make a stable complex with ephrin-B1 via PDZ domain-binding motif -YXV located at the carboxyl terminus of ephrin-B1.[27] It may be important to examine the phosphorylation state of ephrin-B1 *in vivo* in a wide range of cancers to estimate what types of cancers will be sensitive for blocking ephrin-B1 phosphorylation on tumor suppression. For example, phosphorylation of B-type ephrins in invading glioblastoma has been reported recently.[14]

We performed intraperitoneal inoculation of cancer cells into nude mice as a model of peritoneal dissemination of the tumor, as also reported by others.[28,29] Although many gastric cancer cell lines do not show typical histological appearance of human scirrhous carcinoma when inoculated into nude mice, our system of orthotopic transplantation of 44As3 cells is a highly reproducible animal model of peritoneal dissemination of human scir-

Table 2. Dissemination at 15 Days after Orthotopic Implantation of 44As3 Gastric Cancer Cells

Cell	Omentum	Liver	Mesenterium
Mock	7/10 (70)	5/10 (50)	7/10 (70)
4YF	2/11 (18)	1/11 (9)	2/11 (18)

Number of mice bearing tumor at the site per total number of mice bearing tumor (%).

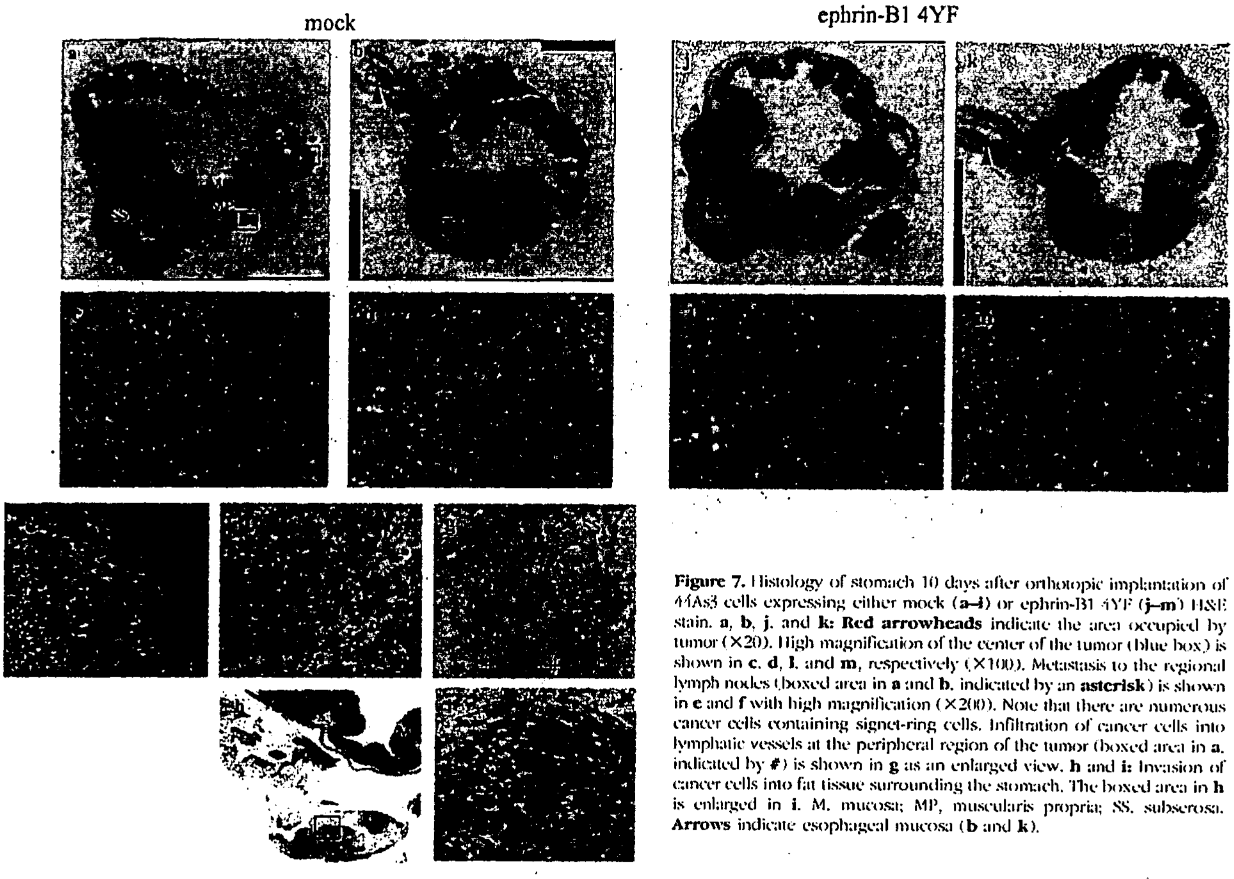

Figure 7. Histology of stomach 10 days after orthotopic implantation of 44As3 cells expressing either mock (**a–i**) or ephrin-B1 4YF (**j–m**) H&E stain. **a**, **b**, **j**, and **k**: **Red arrowheads** indicate the area occupied by tumor (×20). High magnification of the center of the tumor (blue box) is shown in **c**, **d**, **l**, and **m**, respectively (×100). Metastasis to the regional lymph nodes (boxed area in **a** and **b**, indicated by an **asterisk**) is shown in **e** and **f** with high magnification (×200). Note that there are numerous cancer cells containing signet-ring cells. Infiltration of cancer cells into lymphatic vessels at the peripheral region of the tumor (boxed area in **a**, indicated by **#**) is shown in **g** as an enlarged view. **h** and **i**: Invasion of cancer cells into fat tissue surrounding the stomach. The boxed area in **h** is enlarged in **i**. M, mucosa; MP, muscularis propria; SS, subserosa. **Arrows** indicate esophageal mucosa (**b** and **k**).

rhous gastric carcinoma.[18,19,30] Because early clinical diagnosis of scirrhous gastric carcinoma is difficult, peritoneal dissemination or metastasis to lymph nodes has frequently occurred by the time the diagnosis is made. We observed that expression of ephrin-B1 4YF suppressed not only local invasion of 44As3 cells in the gastric wall but also the infiltration of cancer cells into lymphatic vessels and lymph node metastasis. These results suggest that ephrin-B1 phosphorylation-mediated signaling may modulate the process of the invasion of cancer cells to lymphatic vessels. It may be useful to examine the expression and phosphorylation level of ephrin-B1 in a surgical specimen of scirrhous gastric carcinomas to predict lymphatic metastasis of tumors. Dissemination is a frequent form of the recurrence of scirrhous gastric carcinoma, which serves as a major factor determining the prognosis. Ephrin-B1 is considered to be a prognostic factor of gastric scirrhous carcinoma, and the inhibition of a specific cellular signal originating in ephrin-B1 phosphorylation may be a good candidate for regulating its invasion and dissemination.

Table 3. Histological Analysis of the Stomach 10 Days after Orthotopic Implantation of 44As3 Cells

Cell	ly ves	Lymph node	Perforation
Mock	7/10 (70)	7/10 (70)	8/10 (80)
4YF	2/11 (18)	2/11 (18)	3/11 (27)

Data are shown as the number of mice bearing tumor with lymphatic vessel invasion (ly ves), metastasis to regional lymph nodes (lymph node), or perforation of the gastric serosa and infiltrating to the surrounding fat tissue (perforation) per total number of mice bearing tumor (%).

References

1. Blits-Huizinga C, Nelersa C, Malhotra A, Liebl D: Ephrins and their receptors: binding versus biology. IUBMB Life 2004, 56:257–265
2. Murai, KK, Pasquale EB: Ephective signaling: forward, reverse and crosstalk. J Cell Sci 2003, 116:2823–2832
3. Poliakov A, Cotrina M, Wilkinson DG: Diverse roles of Eph receptors and ephrins in the regulation of cell migration and tissue assembly. Dev Cell 2004, 7:465–480
4. Batlle E, Henderson JT, Beghtel H, Van den Born M, Sancho E, Huls G, Meeldijk J, Robertson J, Van de Wetering M, Pawson T, Clevers H: β-Catenin and TCF mediate cell positioning in the intestinal epithelium by controlling the expression of EphB/ephrinB. Cell 2002, 111:251–263
5. Batlle E, Bacani J, Begthel H, Jonkheer S, Gregorieff A, Van den Born M, Malats N, Sancho E, Boon E, Pawson T, Gallinger S, Pals S, Clevers H: EphB receptor activity suppresses colorectal cancer progression. Nature 2005, 435:1126–1130
6. Holmberg J, Genander M, Halford MM, Anneren C, Sondell M, Chumley MJ, Silvany RE, Henkemeyer M, Frisen J: ephB receptors coordinate migration and proliferation in the intestinal stem cell niche. Cell 2006, 125:1151–1263
7. Tanaka M, Kamata R, Sakai R: Phosphorylation of ephrin-B1 via the interaction with claudin following cell-cell contact formation. EMBO J 2005, 24:3700–3711
8. Tanaka M, Kamata R, Sakai R: EphA2 phosphorylates the cytoplas-

mic tail of claudin-4 and mediates paracellular permeability. J Biol Chem 2005, 280:42375–42382
9. Surawska H, Ma PC, Salgia R: The role of ephrins and Eph receptors in cancer. Cytokine Growth Factor Rev 2004, 15:419–433
10. Sawai Y, Tamura S, Fukui K, Ito N, Imanaka K, Saeki A, Sakuda S, Kiso S, Matsuzawa Y: expression of ephrin-B1 in hepatocellular carcinoma: possible involvement in neovascularization. J Hepatol 2003, 39:991–996
11. Meyer S, Hafner C, Guba M, Flegel S, Geissler EK, Becker B, Koehl G, Orso E, Landthaler M, Vogt T: Ephrin-B2 overexpression enhances integrin-mediated ECM-attachment and migration of B16 melanoma cells. Int J Oncol 2005, 27:1197–1206
12. Castellvi J, Garcia A, De la Torre J, Hernandez J, Gil A, Xercavins J, Cajal SR: EphrinB expression in epithelial ovarian neoplasms correlates with tumor differentiation and angiogenesis. Hum Pathol 2006, 37:883–889
13. Varelias A, Koblar SA, Cowled PA, Carter CD, Clayer M: Human osteosarcoma express specific ephrin profiles: implications for tumorigenicity and prognosis. Cancer 2002, 95:862–869
14. Nakada M, Drake KL, Nakada S, Niska JA, Berens ME: Ephrin-B3 ligand promotes glioma invasion through activation of Rac1. Cancer Res 2006, 66:8492–8500
15. Kataoka H, Tanaka M, Kanamori M, Yoshii S, Ihara M, Wang YJ, Song JP, Li ZY, Arai H, Otuki Y, Kobatashi T, Kohno H, Hanai H, Sugimura H: Expression profile of EFNB1, EFNB2, two ligands of EPHB2 in human gastric cancer. J Cancer Res Clin Oncol 2002, 128:343–348
16. Bong YS, Park YH, Lee HS, Mood K, Ishimura A, Daar IO: Tyr-298 in ephrin-B1 is critical for an interaction with the Grb4 adaptor protein. Biochem J 2004, 377:499–507
17. Cowan CA, Henkemeyer M: The SH2/SH3 adaptor Grb4 transduces B-ephrin reverse signals. Nature 2001, 413:174–179
18. Yanagihara K, Tanaka H, Takigahira M, Ino Y, Yamaguchi Y, Toge T, Sugano K, Hirohashi S: Establishment of two cell lines from human gastric scirrhous carcinoma that possess the potential to metastasize spontaneously in nude mice. Cancer Sci 2004, 95:575–582
19. Yanagihara K, Takigahira M, Tanaka H, Komatsu T, Fukumoto H, Koizumi F, Nishio K, Ochiya T, Ino Y, Hirohashi S: Development and biological analysis of peritoneal metastasis mouse models for human scirrhous stomach cancer. Cancer Sci 2005, 96:323–332
20. Akedo H, Shinkai K, Mukai M, Mori Y, Tateishi R, Tanaka K, Yamamoto R, Morishita T: Interaction of rat ascites hepatoma cells with cultured mesothelial cell layers: a model for tumor invasion. Cancer Res 1986, 46:2416–2422
21. Tanaka M, Ohashi R, Nakamura R, Shinmura K, Kamo T, Sakai R, Sugimura H: Tiam1 mediates neurite outgrowth induced by ephrin-B1 and EphA2. EMBO J 2004, 23:1075–1088
22. Kusama T, Mukai N, Tatsuta M, Nakamura H, Inoue M: Inhibition of transendothelial migration and invasion of human breast cancer cells by preventing geranylgeranylation of Rho. Int J Oncol 2006, 29:217–223
23. Blaheta RA, Daher FH, Michaelis M, Hasenberg C, Weich EM, Jonas D, Kolchetkov R, Doerr HW, Cinatl Jr J: Chemoresistance induces enhanced adhesion and transendothelial penetration of neuroblastoma cells by down-regulating NCAM surface expression. BMC Cancer 2006, 6:294
24. Guo DL, Zhang J, Yuen ST, Tsui WY, Chan ASY, Ho C, Ji J, Leung SY, Chen X: Reduced expression of EphB2 that parallels invasion and metastasis in colorectal tumors. Carcinogenesis 2006, 27:454–464
25. Tanaka M, Kamo T, Ota S, Sugimura H: Association of dishevelled with Eph tyrosine kinase receptor and ephrin mediates cell repulsion. EMBO J 2003, 22:847–858
26. Lee HS, Bong YS, Moore KB, Soria K, Moody SA, Daar IO: Dishevelled mediates ephrinB1 signalling in the eye field through the planar cell polarity pathway. Nat Cell Biol 2006, 8:55–63
27. Lin D, Gish GD, Songyang Z, Powson T: The carboxyl terminus of B class ephrins constitutes a PDZ domain binding motif. J Biol Chem 1999, 274:3726–3733
28. Li Z, Zhan W, Wang Z, Zhu B, He Y, Peng J, Cai S, Ma J: Inhibition of PRL-3 gene expression in gastric cancer cell line SGC7901 via micro RNA suppressed peritoneal metastasis. Biochem Biophys Res Commun 2006, 348:229–237
29. Arlt MJE, Novak-Hofer I, Gast D, Gschwend V, Moldenhauer G, Grunberg J, Honer M, Schubiger A, Altevogt P, Kruger A: Efficient inhibition of intra-peritoneal tumor growth and dissemination of human ovarian carcinoma cells in nude mice by anti-L1-cell adhesion molecule monoclonal antibody treatment. Cancer Res 2006, 66:936–943
30. Yanagihara K, Takigahira M, Takeshita F, Komatsu T, Nishio K, Hasegawa F, Ochiya T: A photon counting technique for quantitatively evaluating progression of peritoneal tumor dissemination. Cancer Res 2006, 66:7532–7539
31. Holland SJ, Gale NW, Mbamalu G, Yancopoulos GD, Henkemeyer M, Powson T: Bidirectional signaling through the EPH-family receptor Nuk and its transmembrane ligands. Nature 1996, 383:722–725

JCS ePress online publication date 13 June 2007

The C-terminus of ephrin-B1 regulates metalloproteinase secretion and invasion of cancer cells

Masamitsu Tanaka[1], Kazuki Sasaki[1,2], Reiko Kamata[1] and Ryuichi Sakai[1,*]

[1]Department of Growth Factor Division, National Cancer Center Research Institute, 5-1-1 Tsukiji, Tokyo 104-0045, Japan
[2]Department of Pharmacology, National Cardiovascular Center Research Institute, 5-7-1 Fujishirodai, Suita, Osaka 565-8565, Japan
*Author for correspondence (e-mail: rsakai@gan2.res.ncc.go.jp)

Accepted 28 April 2007
Journal of Cell Science 120, 2179-2189 Published by The Company of Biologists 2007
doi:10.1242/jcs.008607

Summary

Interaction of the Eph family of receptor protein tyrosine kinases and their ligands, ephrin family members, induces bi-directional signaling via cell-cell contacts. High expression of B-type ephrin is associated with high invasion potential of tumors, however, the mechanism by which ephrin-B promotes cancer cell invasion is poorly understood. We show that interaction of ephrin-B1 with the Eph receptor B2 (EphB2) significantly enhances processing of the extracellular domain of ephrin-B1, which is regulated by the C-terminus. Matrix metalloproteinase-8 (MMP-8) is the key protease that cleaves ephrin-B1, and the C-terminus of ephrin-B1 regulates activation of the extracellular release of MMP-8 without requirement of de novo protein synthesis. One possible mechanism by which ephrin-B1 regulates the exocytosis of MMP-8 is the activation of Arf1 GTPase, a critical regulator of membrane trafficking. In support of this hypothesis, activation of ephrin-B1 increased GTP-bound Arf1, and the secretion of MMP-8 was reduced by expression of a dominant-negative mutant of Arf1. Expression of ephrin-B1 promoted the invasion of cancer cells in vivo, which required the C-terminus of ephrin-B1. Our results suggest a novel function of the C-terminus of ephrin-B1 in activating MMP-8 secretion, which promotes the invasion of cancer cells.

Supplementary material available online at
http://jcs.biologists.org/cgi/content/full/120/13/2179/DC1

Key words: Eph, Ephrin, Metalloproteinase, Secretion

Introduction

The members of the Eph receptor family can be classified into two groups based on their sequence similarity and their preferential binding to ligands tethered to the cell surface either by a glycosylphosphatidyl inositol anchor (ephrin-A) or a transmembrane domain (ephrin-B) (Murai and Pasquale, 2003; Blits-Huizinga et al., 2004; Poliakov et al., 2004). The interaction of Eph receptor B2 (EphB2) protein tyrosine kinases and their ephrin-B ligands induces bi-directional signaling via the resultant cell-cell contacts. Ephrin-B has an intracellular domain, which includes sites for tyrosine phosphorylation via Src family kinases and a docking site for proteins with a PDZ domain (Lin et al., 1999; Cowan and Henkemeyer, 2001; Bong et al., 2004). These sites give ephrin-B ligands at least two ways of being involved in intracellular signaling. Although investigation of the functions of Eph receptors and ephrins have focused on the development of the vascular and nervous systems, the roles of Eph-ephrin pathways in epithelial cells and cancers have also attracted interest (Batlle et al., 2002; Klein, 2004; Batlle et al., 2005; Tanaka et al., 2005; Holmberg et al., 2006). Overexpression of B-type ephrin in cancer cells is reported to correlate with high invasion and high vascularity of tumors (Meyer et al., 2005; Castellvi et al., 2006; Nakada et al., 2006), and elevated expression of ephrin-B1 is observed in poorly differentiated invasive tumor cells and other tumors with poor clinical prognosis (Kataoka et al., 2002; Varelias et al., 2002). However, whether ephrin-B actually modifies tumor invasion in vivo has not been established, and the mechanism by which ephrin-B is involved in the invasion of cancer cells is unknown.

Some ephrins are cleaved by a protease. When ephrin-A5 binds with EphA3, their complex creates a recognition motif for a disintegrin and metalloproteinase (ADAM)10 membrane metalloproteinase, which allows effective cleavage of the extracellular domain of ephrin-A5 (Hattori et al., 2000; Janes et al., 2005). Protease-mediated cleavage also occurs for B-type ephrins; a rhomboid transmembrane serine protease RHBDL2 cleaves the transmembrane domain of ephrin-B3 (Pascall and Brown, 2004), and ephrin-B1 and ephrin-B2 are processed within the transmembrane region by the presenilin 1 (PS1)-γ-secretase system to release an intracellular peptide (Georgakopoulos et al., 2006; Tomita et al., 2006).

During the process of screening peptides secreted from pancreas cancer cell lines, we found evidence that the extracellular portion (ectodomain) of ephrin-B1 is secreted. This finding led us to study the mechanism of ephrin-B1 shedding within the ectodomain in cancer cells. In the present study, we show that the C-terminus of ephrin-B1 regulates the exocytosis of MMP-8, a key protease of ephrin-B1 cleavage, in response to the interaction with its receptor EphB2. An accumulating number of reports have shown that increased secretion of metalloproteinases often depends on their transcriptional activation (Chinni et al., 2006; Raymond et al., 2006; Reuben and Cheung, 2006). However, increase of MMP-8 secretion

Journal of Cell Science